PHYSICAL REVIEW A VOLUME 1, NUMBER 3 MARCH 1970

Muonium. I. Muonium Formation and Larmor Precession*

Vernon W. Hughes, Douglas W. McColm,† and Klaus Ziock‡
Gibbs Laboratory, Yale University, New Haven, Connecticut 06520

and

Richard Prepost§
Nevis Laboratory, Columbia University, New York, New York 10027

(Received 14 July 1969)

A complete quantitative discussion is given of the experiments in which muonium was discovered through studies of the depolarization of muons in gases and of the Larmor precession of muonium in argon in a static magnetic field. Also described are the observation of the hfs interval $\Delta\nu$ of muonium in its ground state and the determination of $\Delta\nu$ to an accuracy of about 50% through the use of a static magnetic field. A theoretical discussion is given of muonium formation in gases, including polarization effects. The experimental results on the Larmor precession of muonium prove that close to 100% of the muons stopping in pure argon gas form muonium. The experimental results on muon depolarization in other gases, together with the theoretical considerations, suggest that abundant muonium formation should occur when muons are stopped in most gases; the case of SF_6 appears anomalous in that, at most, only small formation of muonium is indicated. A discussion of the energy levels and decay characteristics of muonium is given. This is the first in a series of papers on the muonium atom and on its interactions in gases.

1. INTRODUCTION

Muonium (μ^+e^-) is the atom consisting of a positive muon and an electron. It is the simplest system involving the muon and the electron; hence its study can yield precise information about the interaction of the muon and the electron. Such information is of particular interest because of the mysterious nature of the muon, which appears to be a heavy electron and occupies an anomalous role in the spectrum of the elementary particles.[1,2] The electromagnetic interaction of the muon and the electron can be studied through measurements of the energy levels of muonium. Weak interactions involving the muon and the electron, such as a coupling of muonium to antimuonium (μ^-e^+), can be studied through observations of the decay of the muon from muonium. Muonium can be regarded as a light isotope of hydrogen, and its collisions with other atoms and molecules, including chemical reactions, can also be studied.

With the discovery of parity nonconservation in the production and decay of the muon,[3,4] it became evident that the essential tool[5] for the study of muonium was available. The decay of a positive pion at rest ($\pi^+ \to \mu^+ + \nu_\mu$) produces a positive muon with its spin in the direction opposite to its linear momentum. Further, the decay of a positive muon ($\mu^+ \to e^+ + \nu_e + \bar{\nu}_\mu$) occurs with an angular asymmetry favoring positron emission in the direction of the muon spin. Polarized muonium can be formed with polarized muons, and the effects of magnetic resonance transitions or collisions in changing muonium-state populations can be observed through the accompanying change in muon polarization, and hence in the angular distribution of the decay positrons.

This is the first in a series of papers on muonium. The initial problem, to which this first paper is devoted, was the formation of polarized muonium in an environment suitable for the study of the properties of muonium. Relatively high-energy polarized positive muons from the decay of positive pions produced with the Columbia University Nevis Synchrocyclotron were stopped in a gas target. First, measurements of the depolarization of muons in various gases were made in order to determine a suitable gas. Then, using pure argon, the formation of polarized muonium in its $1^2S_{1/2}$ ground state was established through the observation of the Larmor precession characteristic of muonium. Finally, a rough measurement of the hfs splitting $\Delta\nu$ of muonium in its ground state was obtained with the use of a static external magnetic field. Brief reports of the research reported here have been published.[6-9]

In its electromagnetic interactions the muon behaves as a Dirac particle with a mass about 207 times that of the electron, according to all present evidence.[2,10,11] Hence the energy levels of muonium should be calculable from the modern quantum electrodynamic theory[12,13] of the electron, muon, and photon fields with the Bethe-Salpeter equation. The hfs interval of the ground state of muonium $\Delta\nu$ has been measured with high precision in a series of experiments in which magnet-

ic resonance transitions were measured at both strong and weak magnetic fields.[9,14-16] The experimental value for $\Delta\nu$ agrees with the theoretical value; indeed, the experimental value can be used to determine the fine-structure constant α which characterizes the strength of all electromagnetic interactions. Three subsequent papers will discuss in detail the experimental determination of $\Delta\nu$ as follows: "Muonium. II. Observation of the Muonium Hyperfine Structure Interval," "Muonium. III. Precision Measurement of the Muonium Hyperfine Structure Interval at Strong Magnetic Field," and "Muonium. IV. Precision Measurement of the Muonium Hyperfine Structure Interval at Weak Magnetic Field."

The interactions of muonium with other atoms and molecules are similar but not identical to the corresponding interactions of hydrogen. Several different methods have been developed for studying these interactions of muonium. Electron spin-exchange collisions with paramagnetic molecules and chemical reactions involving the formation of muonium-containing molecules have been observed, and their cross sections have been determined.[9,17-19] This research will be discussed in "Muonium. V. Interactions of Muonium with Atoms and Molecules."

A limit has been determined for the strength of a weak interaction coupling muonium to antimuonium,[9,20] and this research will be completely reported in "Muonium. VI. Search for Muonium-Antimuonium Conversion."

Since the original discovery of muonium[7] through the studies of muons in gases, which are reported in detail in the present paper, the formation of muonium in some solids and liquids has been observed and the behavior of muonium in condensed matter has been studied by workers in the USSR.[21-23]

2. ENERGY EIGENSTATES; DECAY

The energy levels of muonium given by the nonrelativistic Schrödinger equation are the same as those of hydrogen[13] except for the different reduced mass factor. The ratio[2,24] of the muon mass m_μ to the electron mass m_e is $m_\mu/m_e = (206.761 \pm 0.005)$; hence the Rydberg constant for muonium, R_M, is $R_M = 109\,209.12 \pm 0.02\ \mathrm{cm}^{-1}$, whereas the Rydberg constant for hydrogen,[25] R_H is $R_H = 109\,677.58 \pm 0.01\ \mathrm{cm}^{-1}$. The discrete Schrödinger energy levels of muonium are given by $E_n = -R_M/n^2$, where n is the principal quantum number. Thus the binding energy of the $1^2S_{1/2}$ ground state of muonium is 13.539 eV. The fine-structure splittings of order $\alpha^2 R_M$ are the same as for hydrogen[13] except for the different Rydberg constant.

The ground state of muonium has a hfs interval which is given in first approximation by the Fermi formula[13,26]

$$\Delta\nu = \Delta W/h = \tfrac{16}{3}\alpha^2 cR_\infty \mu_\mu/\mu_B{}^e \simeq 4524\ \mathrm{Mc/sec}, \tag{2.1}$$

in which $\Delta\nu$ is the hfs interval in a frequency unit; ΔW is the hfs interval in an energy unit; α is the fine-structure constant; c is the velocity of light; R_∞ is the Rydberg constant for infinite mass; μ_μ is the muon magnetic moment, and $\mu_B{}^e$ is the electron Bohr magneton ($e\hbar/2m_e c$). Higher-order corrections to this Fermi formula are given in paper II.

The part of the Hamiltonian for muonium which is relevant to our experiments on the ground state is

$$H = a\vec{I}_\mu \cdot \vec{J} + \mu_B{}^e g_J \vec{J} \cdot \vec{H} + \mu_B{}^\mu g_\mu \vec{I}_\mu \cdot \vec{H}, \tag{2.2}$$

in which a is the hfs coupling constant; $\vec{I}_\mu$ is the muon spin operator; $\vec{J}$ is the electron angular momentum operator; g_J is the electron gyromagnetic ratio in muonium ($\simeq +2$); g_μ is the muon gyromagnetic ratio in muonium ($\simeq -2$); $\vec{H}$ is the external static magnetic field; $x = (g_J\mu_B{}^e - g_\mu\mu_B{}^\mu)H/\Delta W$; $\mu_g{}^\mu$ is the muon magneton ($e\hbar/2m_{\hat{\mu}}C$).

The solution for hfs energy levels based on this Hamiltonian is given by the well-known Breit-Rabi formula[27,28]

$$W_{F=\frac{1}{2}\pm\frac{1}{2}, M_F} = -\tfrac{1}{4}\Delta W + \mu_B{}^\mu g_\mu M_F H \pm \tfrac{1}{2}\Delta W(1 + 2M_F x + x^2)^{+1/2}, \tag{2.3}$$

in which F is the total angular momentum quantum number and M_F is the associated magnetic quantum number. Figure 1 shows the energy-level diagram. The weak-field quantum numbers (M_J, M_μ) and the strong-field quantum numbers (M_J, M_μ) are indicated for the four states labeled 1–4.

The spin eigenfunctions $\chi_{F,M_F}(H)$ can be expressed in terms of the strong-field spin eigenfunctions α_μ, β_μ and α_e, β_e:

$$\begin{aligned}
\chi_{1,1}(H) &= \alpha_e\alpha_\mu, \\
\chi_{1,0}(H) &= c\alpha_e\beta_\mu + s\beta_e\alpha_\mu, \\
\chi_{1,-1}(H) &= \beta_e\beta_\mu, \\
\chi_{0,0}(H) &= c\beta_e\alpha_\mu - s\alpha_e\beta_\mu,
\end{aligned} \tag{2.4}$$

in which α_μ, β_μ are the normalized spin eigenfunc-

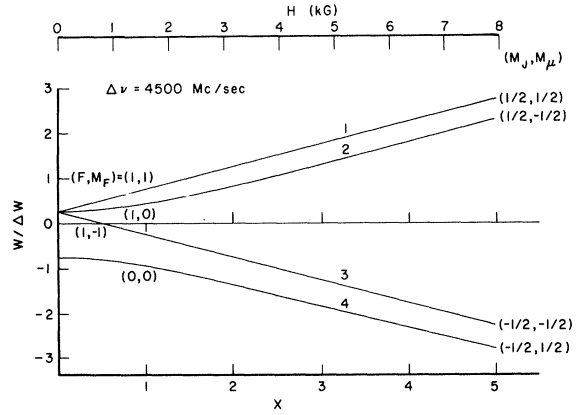

FIG. 1. Energy-level diagram for muonium in its $1^2S_{1/2}$ ground state in a magnetic field, as given by Eq. (2.3). At zero magnetic field the energy difference between the $F=1$ and $F=0$ states is the hfs splitting $\Delta W = h\Delta\nu$.

tions of μ^+; α_μ corresponds to spin orientation along the positive z direction ($M_\mu = +\frac{1}{2}$), β_μ to the opposite spin direction ($M_\mu = -\frac{1}{2}$); α_e, β_e are similarly defined spin eigenfunctions of the electron. The quantities $s(H)$ and $c(H)$ are given by

$$s = (\sqrt{2})^{-1/2}[1 - x/(1+x^2)^{+1/2}]^{+1/2} \ , \qquad (2.5)$$

$$c = (\sqrt{2})^{-1/2}[1 + x/(1+x^2)^{+1/2}]^{1/2} \ ,$$

with $s^2 + c^2 = 1$.

The magnetic moments of the four states are given by the equations

$$\mu_{F,M_F} = -\frac{\partial W_{F,M_F}}{\partial H} \ ,$$

$$\mu_{1/2\pm 1/2,\,0} = \mp 1/2x/(1+x^2)^{1/2}(g_J\mu_B{}^e - g_\mu\mu_B{}^\mu)$$

$$\mu_{1,\,\pm 1} = \mp\tfrac{1}{2}(g_J\mu_B{}^e + g_\mu\mu_B{}^\mu) \ . \qquad (2.6)$$

Muonium is an unstable atom because of the decay of the muon.[2,29] Due to the weak interaction, the positive muon decays with a mean life[2,30] $\tau = (2.1983 \pm 0.0008)\times 10^{-6}$ sec into a positron and two neutrinos:

$$\mu^+ \rightarrow e^+ + \nu_e + \bar{\nu}_\mu \ . \qquad (2.7)$$

Hence, the disappearance of muonium is accompanied by the emission of an energetic positron, two neutrinos, and a low-energy electron. The momentum and asymmetry spectrum or decay probability for the positrons is given with high accuracy upon neglect of terms for radiative corrections and of terms involving m_e/m_μ by the equation

$$N(y,\theta) = 4y^2\{3(1-y) + 2\rho(\tfrac{4}{3}y - 1)$$

$$- P\xi[1 - y + 2\delta(\tfrac{4}{3}y - 1)]\cos\theta\} \qquad (2.8)$$

for positive muons with average polarization P, in which y is the momentum of positron in unit of $\frac{1}{2}m_\mu c$; θ is the angle between the muon spin direction and the positron momentum; ρ is the spectrum shape parameter (Michel parameter) ($=\frac{3}{4}$); ξ is the asymmetry parameter ($=-1$); δ is the energy dependence of asymmetry parameter ($=\frac{3}{4}$). The positron spectrum extends up to a maximum total energy of 52.8 MeV. The positron asymmetry spectrum or angular distribution, $N(\theta)$, is obtained by integrating $N(y,\theta)$ from $y=0$ to 1:

$$N(\theta) \propto 1 - \tfrac{1}{3}A\cos\theta \ , \qquad (2.9)$$

in which $A = P\xi$.

Radiative decay is the only other mode of decay of the positive muon that has been observed:

$$\mu^+ \rightarrow e^+ + \nu_e + \bar{\nu}_\mu + \gamma \ , \qquad (2.10)$$

and it occurs with a relatively small probability corresponding to a branching ratio of order $\alpha[\ln(m_\mu/m_e)]^2$. Another possible mode of disappearance of muonium is the reaction

$$\mu^+ + e^- \rightarrow \nu_e + \bar{\nu}_\mu \ , \qquad (2.11)$$

which is the decay reaction of Eq. (2.7) in which the muonium electron partakes. The probability of this reaction[31] relative to the dominant mode of muon decay [Eq. (2.7)] is about 10^{-10}.

3. THEORY OF MUONIUM FORMATION

Formation of Ground-State Muonium

Since a principal aim of our experiments on muonium is a precise measurement of the hfs interval of the isolated muonium atom and since it is known that the presence of neighboring atoms perturbs the hfs splitting of an atom,[32,33] muonium has been formed and studied in a gas at as low a pressure as possible. In order to avoid chemical reactions and other depolarizing reactions of muonium, which as an isotope of hydrogen and a paramagnetic atom is highly reactive, it was decided to use a pure inert gas (usually argon). For the explicit study of the reactions of muonium with other atoms and molecules (discussed in paper V), these molecules were introduced in small fractional amounts with the argon gas.

Muonium (M) can be formed directly in its ground

state by the capture of an electron from an atom (e.g., argon) by a positive muon:

$$\mu^+ + \mathrm{Ar} \rightarrow \mathrm{M} + \mathrm{Ar}^+ \ . \qquad (3.1)$$

The positive muon enters the gas with an energy up to several MeV and loses energy primarily by ionization and excitation of the gas atoms. Capture and loss of electrons by the muon also occurs and becomes relatively more important at energies below about 15 KeV; indeed some one hundred capture-and-loss reactions occur as the muon is slowed down in the gas.[34] If muonium is stably formed, it will ultimately be thermalized by elastic or inelastic collisions with the gas atoms. It is essential, of course, for the success of experiments on muonium that polarized muonium be stably formed.

Clearly, the history of a muon stopping in a gas is a most complex process, involving many types of atomic collisions for the positive muon and for muonium. No detailed theoretical treatment of the over-all problem has been attempted, primarily because of the lack of quantitative knowledge about many of the cross sections involved. However, we present below some theoretical and experimental information on charge-capture and loss cross sections and then further discussion of the over-all problem.

An energy-level diagram which is useful for a discussion of muonium formation is shown in Fig. 2. With reference to helium the zero-energy level for an electron is taken to be that of an electron bound in the ground state of helium. The ionization energy of helium $E_I(\mathrm{He})$ is 24.58 eV and that of muonium $E_I(\mathrm{M})$ is 13.54 eV. Hence, in order that a muon can capture an electron from a helium atom to form muonium in its ground state, the kinetic energy of the muon-helium system in its c.m. coordinate system must be greater than the threshold value

$$E_t = E_I(\mathrm{He}) - E_I(\mathrm{M}) \ , \qquad (3.2)$$

which equals 11.04 eV. In the laboratory coordinate system with the helium atom initially at rest, the kinetic energy of the muon required for muonium formation is given by

$$E_t(\mathrm{Lab}) = E_t m_\mu / m_r \ , \qquad (3.3)$$

in which $m_r = m_\mu m_{\mathrm{He}}/(m_\mu + m_{\mathrm{He}})$, where m_{He} is the mass of a helium atom. Hence the threshold kinetic energy of the muon is $E_t(\mathrm{Lab}) = 11.35$ eV. If the muon-helium system has a kinetic energy less than 11.04 eV, it is in energy region IV below the muonium formation threshold. If the muon-helium system is in energy region III with kinetic energy between 11.0 and 19.8 eV, no other inelastic collision process than muonium formation is energetically possible. In energy region II, above the first excited state of He, excitation of discrete states of He by the muon is energetically possible. In energy region I, ionization of He can occur. Formation of muonium in its excited $n = 2$ state by a charge-capture reaction will require a kinetic energy for the muon-helium system of 21.2 eV.

Figure 2 also shows the corresponding energy-level diagram for argon, where the threshold energy for muonium formation is $E_t = 2.2$ eV. The values of E_t for the rare gas atoms and for some molecules are given in Table I. For Xe and several molecules, the electron-capture reaction is endothermic.

The theory of the charge-capture reaction as an example of a rearrangement collision[35] has received much attention since the early days of the

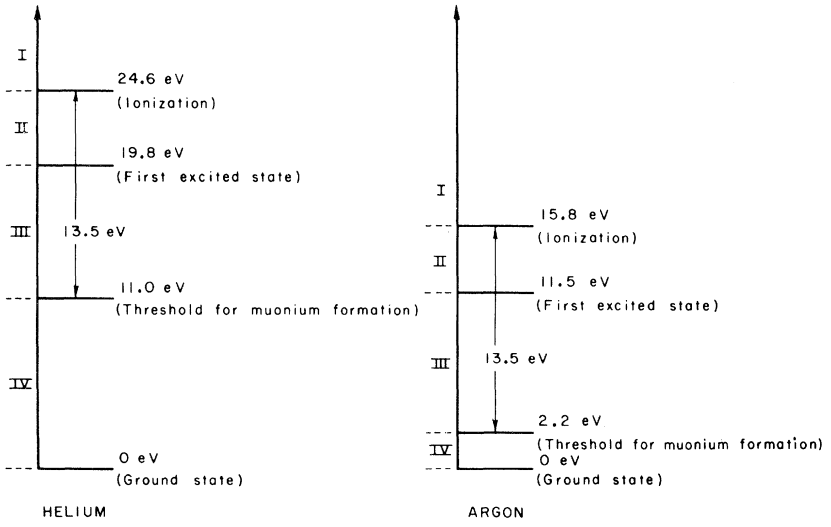

FIG. 2. Energy-level diagram relevant to muonium formation in helium and argon.

TABLE I. Threshold energies E_t for muonium formation.

Atom or molecule	E_t(eV)
He	+11.04
Ne	+8.02
Ar	+2.22
Kr	+0.46
Xe	−1.41
O_2	−1.3
N_2	+2.0
N_2O	−0.6
SF_6	~+3 [a]

[a] J. D. Craggs and H. S. W. Massey, Encyclopedia of Physics, edited by S. Flügge (Springer-Verlag, Berlin, 1959), Vol. 37/1.

quantum theory of atomic collisions, but accurate values for inelastic charge-capture cross sections have not been calculated, due the the mathematical complexity of the problem. However, the general features of the charge-capture cross section involved in muonium formation can be predicted theoretically.[35–38] Since the mass of the muon is 207 times the mass of the electron, the muon can

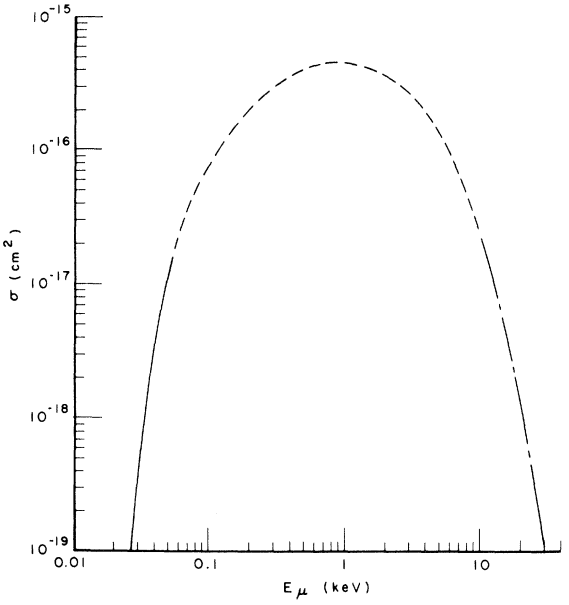

FIG. 3. Calculated capture cross section for the reaction $\mu^+ + He \rightarrow M + He^+$, in which muonium M is formed in its ground state by electron capture from helium, as a function of muon kinetic energy E_μ. The three portions of the theoretical curve are based on the following theoretical approximations: (1) ———, at low energy E_μ, the adiabatic approximation or the PSS method. (2) ----------, at intermediate energy E_μ, an impact-parameter method. (3) — - — - —, at high energy E_μ, a Born approximation.

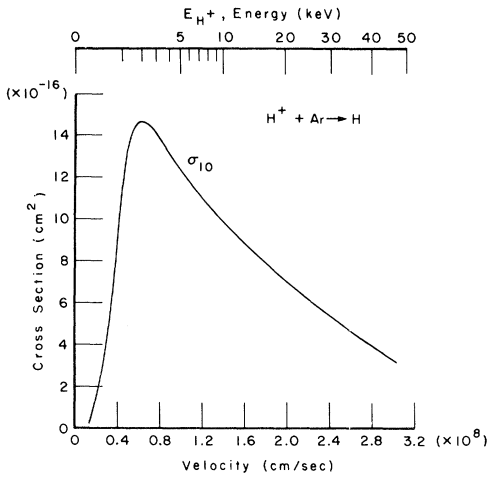

FIG. 4. Measured cross section for the reaction: $H^+ + Ar \rightarrow H$ in which hydrogen is formed by electron capture from argon, as a function of the velocity or kinetic energy of the incident proton.

be treated as a heavy particle similar to the proton in atomic reactions. In the so-called adiabatic region above the threshold energy, the capture cross section for a reaction such as (3.1) rises rapidly with muon kinetic energy E_μ, and has approximately an exponential dependence on the inverse of the muon velocity. The cross section has a relatively flat maximum for muon velocities v_μ which satisfy the condition

$$a\,|\Delta E|/\hbar v_\mu \simeq 1, \tag{3.4}$$

where $|\Delta E|$ is the magnitude of the change in internal energy involved in the reaction ($|\Delta E| = 2.2$ eV) and a is a distance parameter which characterizes the range of the muon-atom interaction potential ($a \simeq 8 \times 10^{-8}$ cm). In the high-energy region the cross section decreases monotonically towards zero with increase in E_μ with a high inverse power of v_μ.

Theoretical estimates of the cross section for muonium formation in its ground state have been made for the case of electron capture from helium:

$$\mu^+ + He \rightarrow M + He^+ \ . \tag{3.5}$$

The results shown in Fig. 3 agree with the general features of the capture cross section just described. A discussion of the calculation is given in Appendix A.

The best information available on charge-capture reactions relevant to muonium formation in gases is obtained from experimental data on charge-capture reactions of protons to form hydrogen atoms. For most of our work, argon has been used as the gas in which muonium is formed and studied. Figure 4 shows the measured capture cross section for

the reaction[38–44]

$$H^+ + Ar \rightarrow H \ . \qquad (3.6)$$

The measurements yield the total cross section for producing neutral H, including its excited states, and do not determine the final charge state of the argon ion. Direct capture into the ground state probably accounts for about 0.9 of the total cross section. From our theoretical understanding of the charge-capture reaction we know that the cross-section curve for the corresponding muon charge-capture reaction will be similar in form to Fig. 4, and the cross-section values will be approximately equal when the velocity of the muon equals the velocity of the proton.

Muonium in its ground state is only one of several atomic or molecular species in which the muon can occur before it decays. Firstly, the muon could remain unattached as a positive muon in the gas. Secondly, it could attach to a gas atom to form a positive molecular ion such as μ^+Ar.[45, 46] Thirdly, various muonium-containing molecules could be formed. The relative probabilities for these different species depend on the cross sections of all the reactions involved in the relevant energy range extending from several MeV, at which the muon enters the gas, down to thermal energy; many of these cross sections are not known even to within 1 or 2 orders of magnitude.[44]

Information relevant to the question of what fraction of the muons stopping in a gas will form muonium is provided by measurements of the equilibrium charge states of protons passing through a gas. Figure 5 shows experimental data on the equilibrium fractions of the beam in the charge states H^+, H, and H^- (F_{+1}, F_0, and F_{-1}, respectively) as a function of beam kinetic energy for protons in argon.[40, 42, 47] The ratio of the fraction of the beam in the charge state +1 to that in 0, F_1/F_0, at a given energy is approximately equal to the ratio of the cross sections for ionization and charge capture, σ_{01}/σ_{10}. The measurements determine only the charge state of the proton; therefore for the neutral form H do not establish directly that H is in its ground state; however, in view of the shortness of the lifetime of most excited states and the relatively small cross sections for electron capture into excited states, the neutral form is very probably almost entirely in the ground state. It is seen that at a kinetic energy of 5 keV a fraction of the beam greater than 0.9 is in the neutral state H. Hence we can expect that for protons stopped in argon close to 100% will exist as H.

Although experimental data for muons in argon corresponding to those for protons in argon shown in Figs. 4 and 5 are not known, it can be expected, as mentioned above, that the muon and muonium cross sections will be about the same as the H^+ and H cross sections at the same velocities. Hence,

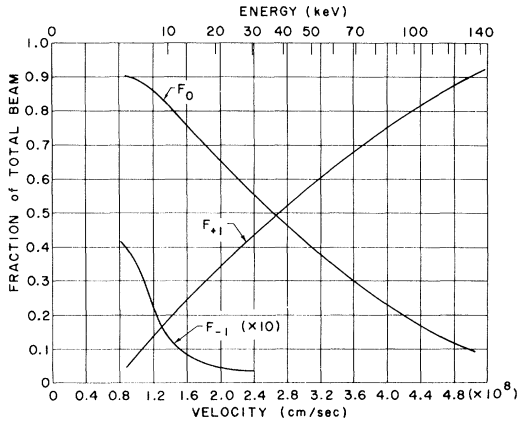

FIG. 5. Measured equilibrium fractions of the hydrogen charge states H^+, H, and H^- (F_{+1}, F_0, and F_{-1}) in argon as a function of hydrogen velocity or kinetic energy.

essentially 100% of the muons stopping in argon gas will be in the ground state of muonium. Indeed this same conclusion, that there is a very high probability for muons stopped in a gas to form muonium, will apply to all the rare gases, and probably to most other gases where muonium containing molecules are not formed.

The time interval between the entrance of a high-energy muon of several MeV kinetic energy into the gas and the formation and thermalization of a muonium atom is of some importance to our experiments. The slowing-down time t_1 from the entrance of the muon to the formation of muonium with a kinetic energy of about 1 keV is of the order of 10–50 nsec for an argon gas pressure of 50 atm, where the muon travels about 10 cm. The thermalization of the muonium atom occurs principally through elastic collisions with argon atoms. If we assume that the elastic scattering cross section[48] σ is independent of the kinetic energy of the muonium atom and is principally s-wave scattering and that the fractional muonium kinetic energy loss per collision is $2\,m_\mu/m_{\mathrm{Ar}}$, then the thermalization time t_2 is given by the equation

$$t_2 = \frac{m_{\mathrm{Ar}}}{2^{1/2} n\sigma\, m_\mu^{1/2}} \frac{1}{E_{\mathrm{M}}^{1/2}} \Bigg|_{E_{\mathrm{M}}(\mathrm{initial})}^{E_{\mathrm{M}}(\mathrm{thermal})} . \qquad (3.7)$$

Taking $\sigma = 10^{-15}$ cm^2, $n = 1.4 \times 10^{21}$ Ar atoms/cm^3, $E_{\mathrm{M}}(\mathrm{initial}) = 1$ keV, and $E_{\mathrm{M}}(\mathrm{thermal}) = 0.04$ eV, we obtain $t_2 = 3.1 \times 10^{-10}$ sec. We note that $t_2 \ll t_1$ and that the total slowing-down time $t_1 + t_2$ is small compared to the muon mean lifetime of 2.2 μsec.

It is perhaps useful to make a few remarks about the comparison of positronium and muonium formation. Since the masses of the muon and proton are both much greater than the mass of the electron or

positron, the Born-Oppenheimer approximation for the treatment of collision processes will apply almost equally well for the muon and the proton, but not for the positron. Hence the behaviors of muonium and of hydrogen are very similar, whereas that of muonium and of positronium are not. Thus the substantial information known[49-51] about the formation and behavior of positronium in gases has only limited applicability to muonium problems.

Formation of Polarized Muonium

Since the incident muons are polarized because of their origin from pion decay, muonium atoms are formed with a net polarization. Indeed it is essential for all our experiments on muonium that the muonium atoms be polarized, as will be made clear later in this paper and in subsequent papers. A simplified description of the polarization phenomena is the following: In the frame of reference of a π^+ meson at rest, the decay μ^+ has its spin direction opposite to the direction of its linear momentum. The beam transport system selects muons which decay in the laboratory frame of reference in the direction of the pion beam; hence, in the laboratory frame, the muons are highly polarized in the direction opposite to their momentum. The slowing down of the muons in matter does not alter their polarization direction. Furthermore, since the charge-capture reaction by which muonium is formed is predominantly caused by the Coulomb interaction, the polarization of the muons is not changed in the process of muonium formation. Once muonium is formed, however, the magnetic interaction between the muon spin magnetic moment and the electron spin magnetic moment can alter the muon spin direction and thus leads to a partial depolarization of the muons.

For a more detailed quantitative discussion of the polarization phenomena we note first that for the π^+ decay

$$\pi^+ \rightarrow \mu^+ + \nu_\mu \,, \tag{3.8}$$

the muon helicity in the π^+ rest frame is expected theoretically[29] to be -1, and several experiments have confirmed[52-54] this expectation to an accuracy of about 30%.

If the π^+ meson has a momentum p_π in the laboratory frame (whose z axis is taken opposite to the direction of p_π), the μ^+ momentum p_μ in the laboratory frame is given by the expression

$$\begin{aligned} cp_{\mu z} &= (1-\beta_\pi^2)^{-1/2}(cp'_\mu \cos\theta' + \beta_\pi E'_\mu)\,, \\ p_{\mu x} &= p'_{\mu x}\,, \\ p_{\mu y} &= p'_{\mu y}\,, \end{aligned} \tag{3.9}$$

where primed quantities refer to the π^+ rest frame and unprimed quantities refer to the laboratory frame; β_π is the normalized velocity v_π/c of the pion; θ' is the polar angle of emission of the muon in the pion rest frame (z' axis is parallel to z axis). The quantities p'_μ and E'_μ (total muon energy) have the values $p'_\mu = 29.8$ MeV/c and $E'_\mu = m_\mu c^2 + 4.12 = 109.78$ MeV. The muon spin direction is defined only in the muon rest frame.[55] If we choose the z'' axis of the muon rest frame (designated by double primed quantities) opposite to the polar direction θ' of muon emission with respect to the pion rest frame, then the muon spin will be in the positive z'' direction in the muon rest frame or in the polar direction $\pi - \theta'$.

The muon spin direction is known to be substantially unaffected when a relatively high-energy muon is slowed down in matter,[56,57] because principally the Coulomb interaction is involved and the magnetic forces are small. Hence the muon polarization will depend on the characteristics of the beam transport system which will determine the range of muon momenta p_μ and muon decay angles θ' present in the muon beam. In practice for our experimental arrangement (see Sec. 4) the polarization P

$$P = 2\langle I_{\mu z}\rangle \tag{3.10}$$

of the slow muon beam is greater than +0.8.

Polarized muonium will be formed when a polarized muon captures an atomic electron from an unpolarized atom. The distribution of muonium atoms in the four hfs magnetic substates depends on the initial polarization of the muons and on the magnetic field $\vec{H}$. If $P = +1$ and $\vec{H}$ is in the z direction, then the probabilities p_i of forming the hfs substates are given by

$$p_1 = \tfrac{1}{2}; \quad p_2 = \tfrac{1}{2}s^2; \quad p_3 = 0; \quad p_4 = \tfrac{1}{2}c^2; \tag{3.11}$$

in which the state designations i are those given in Fig. 1 and the quantities s and c are given in Eq. (2.5). The formation of muonium can lead to a partial depolarization of the incident muons, and from (3.11) it follows that the resulting polarization P of the muons forming muonium is given by

$$P = \tfrac{1}{2} + \tfrac{1}{2}x^2/(1+x^2)\,, \tag{3.12}$$

in which x is defined for Eq. (2.2). A discussion of the derivation of Eqs. (3.11) and (3.12) is given in Appendix B.

In slowing down in a gas, a muon may partake in many charge capture-and-loss reactions. If the lifetime of the muonium state is much longer than $1/\Delta\nu$, then in each muonium formation the muon polarization will be reduced by the factor P of Eq. (3.12). This process has been considered in con-

nection with the observations of the depolarization of muons in solids.[58, 59]

4. DEPOLARIZATION OF MUONS IN GASES

The search for muonium formation in gases first involved a study of the depolarization of muons stopped in various gases [6, 60] in an experiment similar to the original experiment in which muon precession in a magnetic field was observed.[56] The motivation for this study was the following: The magnetic moment of a free muon is μ_μ and its Larmor precession frequency in a magnetic field H is[61]

$$f_{L\mu} = 2\mu_\mu H/h = 13.5 H \text{kc/sec} \quad (H \text{ in gauss}). \tag{4.1}$$

The magnetic moment of muonium depends on the hfs magnetic substate and on H [see Eq. (2.6)]; under weak-field conditions, where the magnetic interaction with the external magnetic field is small compared to the hfs interaction or $x \ll 1$, the magnetic moments μ_i become approximately

$$\mu_1 \simeq -\mu_B^e; \qquad \mu_2 \simeq -x\mu_B^e;$$
$$\mu_3 \simeq +\mu_B^e; \qquad \mu_4 \simeq +x\mu_B^e. \tag{4.2}$$

The Larmor precession frequency for muonium in the states 1 and 3 in a weak magnetic field is approximately

$$f_{LM} \simeq \mu_B^e H/hF = \mu_B^e H/h = 1.40H \text{ Mc/sec}, \tag{4.3}$$

since the triplet state has $F = 1$. The induced magnetic moments of states 2 and 4 are about $\frac{1}{4}\mu_\mu$ at the magnetic fields H used in this experiment. If muons remain free in the gas, then muon precession at the free-muon precession frequency $f_{L\mu}$ should be observed in the experiment. On the other hand, if the muons form muonium, then the characteristic muonium precession frequency f_{LM}, which is about 100 times larger than $f_{L\mu}$, should be observed. Hence the absence of an observed free-muon precession is a necessary condition for the abundant formation of muonium.

Experimental Method and Apparatus

The method of the experiment[56] was to measure the effective asymmetry parameter of the decay positron angular distribution by the technique of observing the positron counting rate with a fixed-counter telescope as a function of time when a magnetic field is applied. A schematic diagram of the experimental arrangement is shown in Fig. 6. With the coordinate axes as shown, the initial muon polarization is in the positive z direction, the applied static magnetic field is in the x direction, and the positron counter telescope (counters 4 and 5) is located in the y direction. With reference to Eq. (2.9) the positron angular distribution from muon decay is given by

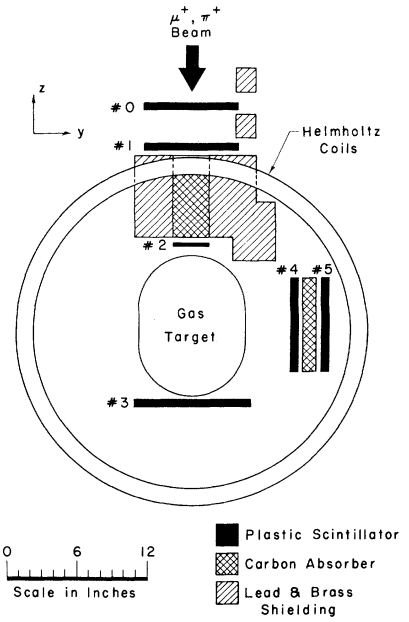

FIG. 6. Schematic diagram of the experimental arrangement used for the study of the depolarization of muons in gases and of the Larmor precession of muonium.

$$N(\theta) \propto 1 + a\cos\theta, \tag{4.4}$$

$$a = \tfrac{1}{3}P(1 - D), \tag{4.5}$$

in which θ is the angle between the direction of the positron momentum and that of the muon spin, a is the asymmetry parameter, P is the initial polarization of the muons in the incident beam, and D is the depolarization factor by which the initial muon polarization is reduced by moderation in the absorber and the gas. In the magnetic field H the muon spin will precess with the Larmor frequency $f_{L\mu}$ of Eq. (4.1); hence the positron angular distribution will rotate with this frequency. Measurements are made of the positron counts during time intervals which correspond to sampling the maximum (peak) and minimum (valley) of the distribution.

Muon Beam, Detectors, and Magnetic Field

The muon beam was produced from the 380-MeV proton beam of the Columbia University Nevis

Synchrocyclotron. The beam from an internal target was momentum selected in the range of 190 MeV/c ± 10% by the fringing field of the synchrocyclotron magnet and by an external dipole magnet. (During a portion of the experiment a quadrupole lens was used upstream from the dipole magnet.) The composition of this beam was about 10% muons and 90% pions. A brass collimator with a 3 × 3-in. opening was placed between scintillation counters 1 and 2, and enough carbon absorber was inserted in the opening so that pions stopped before counter 2 and muons stopped in the target between counters 2 and 3. Range curves indicated that the composition of the beam stopping in the target was about 80% muons and 20% pions, and the width of the stopped muon beam was equivalent to about 3.8 g/cm^2 of carbon.

The incoming beam and the decay positrons from positive muons were detected with plastic scintillation counters viewed by 6810A photomultiplier tubes, which were magnetically shielded by concentric layers of Mumetal, Netic-Co-Netic[62] metal, and soft iron. A coincident 12 and anticoincident $\bar{3}$ count, designated $12\bar{3}$, indicated a particle stopping in the target (or in counter 2) or being scattered out of the beam. A subsequent coincident 45 count but anticoincident 2 count, $(45\bar{2})$, indicated a decay positron. The $12\bar{3}$ pulse was used to generate a gate pulse delayed by 0.4 μsec and having a width of 1.4 μsec, and a so-called event pulse was generated when a $45\bar{2}$ pulse was coincident with a gate pulse. Standard pulse electronics circuitry[63-65] employing principally 6922 and 6688 vacuum tubes was used and provided a coincidence resolution time of about 10 nsec. With the gas target to be described, typical counting rates for $12\bar{3}$ counts were 100 sec^{-1} and for events were 2 sec^{-1}.

The magnetic field for precession of the muon magnetic moment was provided by a pair of 30-in.-diam coils lying in horizontal planes spaced by 15 in. (Helmholtz coils). The current was supplied by a full wave bridge rectifier filtered by storage batteries. A field of +17 G (up) or −17 G (down) was used, and with this magnitude of field the free-muon spin precesses through 90° in 1.1 μsec, the midtime of the gate. The magnetic field was homogeneous over the gas target to within about 2% total variation. Data were taken in 20-min runs alternately with fields of +17 G and −17 G in order to measure the peak and valley of the positron angular distribution.

Gas Target

The target vessel was made from two stainless-steel (type 302) hemispheres of 9 in. diam with a thickness of 0.065 in. and a straight cylindrical section of 0.070-in. thickness (0.7 g/cm^2), so that the over-all length was 12 in. It was assembled by heliarc welding and tested to 1500 psi. The actual pressures used ranged 180–900 psi. The vessel had two connectors for gas handling and could be evacuated with a mechanical and an oil diffusion pump to a pressure of 10^{-5} Torr before filling with gas.

TABLE II. Stopping gases and their purities.

Gas	Purity[a]
O_2	>99.5%
N_2	>99.8%
SF_6	>98%
N_2O	>98%, with air as major impurity
Ar (Linde, Inc.)	Total impurity concentration (except for noble gases) < 20 ppm, with < 7 ppm N_2, < 4 ppm O_2, and < 6 ppm H_2O
Ar (continously purified)	See Sec. 5

[a]As specified by manufacturer.

The gases used and their purities are indicated in Table II. The last entry refers to argon gas that is continuously purified during the experiment, as will be discussed in Sec. 5, where it was vitally important for the direct observation of muonium.

Dummy Target

Since about one-half of the muons stopped in the walls of the target vessel and hence provided background events, it was necessary to make measurements with a dummy target in order to obtain the information needed to correct for wall background events and hence to determine the asymmetry parameter a for the gas alone. It was not possible to correct for wall background simply by taking data with the target vessel evacuated, because the presence of the gas affects importantly the number and spatial distribution of muons stopping in the walls.

The dummy target is shown in Fig. 7. It consisted of a stainless-steel vessel similar to the gas-target vessel which could be disassembled. An assembly consisting of 18 aluminum sheets, each 0.020 in. thick, uniformly spaced and held together with Styrofoam spacers, could be inserted in the dummy vessel. The over-all thickness of the aluminum plates was 2.4 g/cm^2. Aluminum was chosen because its atomic number Z is 13 and hence close to that of argon (Z = 18), which was the gas we were particularly interested in studying.

With this dummy target it was possible to determine the asymmetry coefficient a for the gas alone by making peak and valley measurements for the following conditions: (1) Gas target, filled with gas to a stopping power equal to that of 2.4 g/cm^2 of Al. (2) Dummy target, completely assembled.

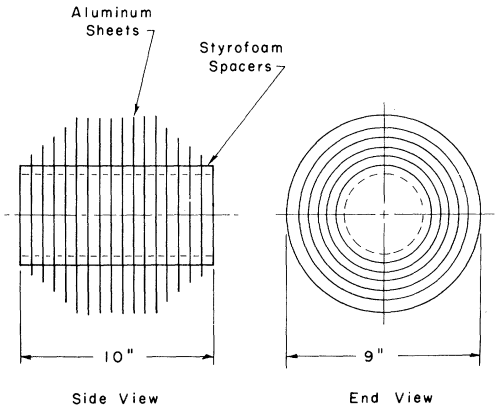

FIG. 7. Dummy target used for the study of the depolarization of muons in gases. Only the internal assembly consisting of aluminum and styrofoam is shown.

(3) Assembly of Al sheets only. Two 0.070-in. stainless-steel plates, one upstream of counter 2 and the other between counters 4 and 5. (4) No target.

Data and Data Analysis

For each of the gases listed in Table II, peak and valley events were measured for conditions (1)–(4), as indicated above. The total number of counts of peak and valley events amounted to about 1000 for conditions (1)–(3), and about 50 for condition (4). These figures corresponded to stopping about 50 000 muons for each gas studied.

In addition, in order to be able to obtain the gas asymmetry parameter relative to that of carbon (graphite) as a standard, measurements of peak and valley events were made for aluminum and for carbon using $3 \times 3 \times 1$-in.-thick targets, which provided a very good geometry.

The analysis of the data to obtain the gas asymmetry parameter is based on the following equations: For the condition (1) with the gas target,

$$N_+^1 = N_g(1+SGa_g)+N_w(1+SGa_w)+N_2(1+SGa_2)\,,$$
$$N_-^1 = N_g(1-SGa_g)+N_w(1-SGa_w)+N_2(1-SGa_2)\,, \tag{4.6a}$$

in which N_+^1 are the events counts ($45\bar{2}$ counts during delayed 1.4-μsec gate time) with magnetic field H in the up direction. N_-^1 are the events counts with H down. The incident-beam intensity was monitored by the coincident 01 counts, designated by N_0, and the N_+ and N_- events counts were observed for the same number of N_0 monitor counts. Indeed all the observed events counts given in Eqs. (4.6a) are normalized to the same N_0 value. N_g are the events counts from the gas alone with $H = 0$; N_w are the events counts from the walls alone with $H = 0$; N_2 are the events counts from counter 2 alone with $H = 0$; a is the asymmetry parameter; $S = \sin\Delta\theta/\Delta\theta$, in which $2\Delta\theta$ is the effective total angle in the yz precession plane subtended at the target by the 45 counter telescope; $2\Delta\theta \simeq 0.8$ rad. The quantity S can be considered as a correction factor associated with the angular acceptance of the 45 counter telescope. We have

$$G = \int_{t_D}^{t_D+t_G} e^{-t/\tau}\cos(\tfrac{1}{2}\pi - \omega t)\,dt \times\left(\int_t^{t_D+t_G} e^{-t/\tau}dt\right)^{-1}\,,$$

where τ, the muon mean life, $= 2.2$ μsec; t_D, the gate delay time, $= 0.4$ μsec; t_G, the gate width, $= 1.4$ μsec; ω, the muon angular precession frequency, $= 1.4\times10^6$ rad sec^{-1} for $H = +17$G. For $H = +17$G, $G = 0.84$. The quantity G can be regarded as a correction factor associated with the finite width of the gate pulse. For the condition (2) with the dummy target, we obtain

$$N_\pm^2 = N_{\mathrm{Al}}(1 \pm SGa_{\mathrm{Al}}) + N_w(1 \pm SGa_w) + N_2(1 \pm SGa_2), \tag{4.6b}$$

in which N_{Al} are the events counts from the aluminum alone with $H = 0$. For the condition (3) with the Al assembly alone, we obtain

$$N_\pm^3 = N_{\mathrm{Al}}(1 \pm SGa_{\mathrm{Al}}) + N_2(1 \pm SGa_2). \tag{4.6c}$$

For the condition (4) with no target,

$$N_\pm^4 = N_2(1 \pm SGa_2). \tag{4.6d}$$

It is implicit in these formulas that N_w has the same value in conditions (1) and (2), and that S and G are the same values throughout.

Using Eqs. (4.6) an expression can be derived for a_g/a_{Al} in terms of measured quantities

$$\frac{a_g}{a_{\mathrm{Al}}} = \frac{(N_+^1 - N_+^2) - (N_-^1 - N_-^2) + (N_+^3 - N_+^4) - (N_-^3 - N_-^4)}{(N_+^1 - N_+^2) + (N_-^1 - N_-^2) + (N_+^3 - N_+^4) + (N_-^3 - N_-^4)} \times \frac{(N_+^3 - N_+^4) + (N_-^3 - N_-^4)}{(N_+^3 - N_+^4) - (N_-^3 - N_-^4)}\,. \tag{4.7}$$

From the measured quantities we can also deter-

mine that $N_g \simeq 0.7N_w$ and $N_2 \simeq 0.1N_g$.

Analysis of the measurements to compare aluminum and carbon, which involved measurements analogous to those of Eqs. (4.6a) and (4.6b), yielded for the ratio of the asymmetry parameters the result

$$a_{Al}/a_C = 0.96 \pm 0.05, \tag{4.8}$$

in which the error is 1 standard deviation and is due to counting statistics and background corrections. After taking into account calculated values of S and G and background corrections, we obtained

$$a_C = 0.31 \pm 0.02. \tag{4.9}$$

This value is consistent with $P = 0.9$ and $D = 0$ in Eq. (4.5). The carbon absorber between counters 4 and 5 provided a low-energy cutoff for positrons in the 45 counter telescope of about 10 MeV; this cutoff changes the theoretically predicted numerical asymmetry factor in Eq. (2.9) from 0.333 to 0.335, which is only a small change. This measured value for a_C is consistent with other experimental results.[66,67]

The principal error involved in determining a_g/a_{Al} from Eq. (4.7) is the statistical counting error for the many measured quantities. However, several sources of systematic errors were investigated and some of these were appreciable. One important systematic error arose from multiple scattering. Differences in multiple scattering from the gas and from the Al sheets made the wall background subtraction with the dummy target inaccurate, principally because different numbers of muons were scattered into the side walls for the gas target [condition (1)] and for the dummy target [condition (2)]. Also for condition (3) particularly, muons can be scattered and stop in counter 4. Calculations of multiple scattering based on formulas for mean scattering angle as a function of range[68,69] indicate that about $(10 \pm 3)\%$ of the muons scatter into the side walls for conditions (1) and (2) and out of the Al assembly for condition (3). This result implies that an error of about 10% is made in the determination of N_w/N_g and hence an error of about 5% in a_g/a_{Al}. The effect of multiple scattering on S is negligibly small. Errors associated with accidental counts and instabilities in the electronics were negligible.

Results and Discussion

The results for the asymmetry parameters of the gases relative to that of carbon (graphite) a_g/a_C are shown in Table III. Except for the case of SF_6 and possibly also of O_2, the values are low and hence indicate that free polarized muons do not exist in these gases. This result is a necessary but not a sufficient condition that muonium is formed in these gases with low values of a_g/a_C. Particularly for SF_6 it appears that effectively free polarized muons may exist in the gas. In view of our discussion in Sec. 3 it might be expected that muonium would be formed in all gases; hence this result for SF_6 is a bit surprising.

TABLE III. Asymmetry parameters for gases relative to that for carbon (graphite).[a]

Gas	a_g/a_C
O_2	0.44 ± 0.21
N_2	0.13 ± 0.22
SF_6	0.75 ± 0.21
N_2O	0.10 ± 0.20
Ar (Linde, Inc.)	0.22 ± 0.20
Ar (continuously purified)	0.08 ± 0.15

[a]Purities of the gases are given in Table II. The errors indicated are 1 standard deviation and due principally to counting statistics.

5. LARMOR PRECESSION OF MUONIUM

The absence of a free-muon Larmor precession signal for muons stopped in a gas is a necessary condition for abundant muonium formation in the gas, but it does not constitute a proof that muonium is formed, and even more so, it does not prove that polarized muonium is formed. Although it is reasonably well established that polarized muons are not appreciably depolarized by the inelastic collisions of ionization and excitation of gas atoms by means of which the muons are slowed down (Sec. 3), various possibilities can be considered by which muon polarization can be lost when atomic and molecular species involving the muon are formed at relatively low kinetic energies. If polarized muonium is formed, it may become depolarized in collisions with other atoms or molecules; in particular, an electron spin-exchange collision with a paramagnetic atom or molecule can lead to a change in muon polarization through the muonium hfs interaction.[19,70,71] The formation of a molecular ion involving the muon may lead to depolarization of the muon through the spin-rotation interaction in the molecule.[45]

After the experiment described in Sec. 4 on the depolarization of muons in gases, the next experiment undertaken[72] was a direct search for a Zeeman transition in muonium induced by an rf magnetic field. The transition looked for was $(F, M_F) = (1, \pm 1) \leftrightarrow (1, 0)$ in a static magnetic field of 4 G, with an rf frequency of about 5.6 Mc/sec. The gas used was N_2O, because of the low value observed for a_g/a_C for N_2O (see Table III). The

static magnetic field $\vec{H}_0$ was opposite to the direction of the incident muon beam (positive z direction) and the rf field $\vec{H}_{rf}$ was perpendicular to $\vec{H}_0$. Decay positrons were observed along the $-z$ direction. If the muonium Zeeman transition were induced by the rf field, the decay positron angular distribution would be altered, and a change would be observed in the number of decay positrons in the $-z$ direction due to the presence of the rf field. For this experiment the stainless-steel gas container was replaced by a Fiberglas Epoxy container in order that the rf field could be applied from outside the container. No change was observed in the number of decay positrons due to the rf field; hence there was no indication of muonium formation. In retrospect, it is not at all surprising that no muonium was observed in this experiment. It is probable that polarized muonium was formed when the muons stopped in N_2O, but that the muonium atoms then rapidly lost their polarization in collisions with the paramagnetic N_2O molecules.[19]

In view of the negative result in the search for muonium in N_2O and of our explanation that this was due to depolarizing collisions of muonium with N_2O, we planned to search for muonium by stopping muons in a nonreactive and pure rare gas – argon. Furthermore, it was decided to look directly for the Larmor precession frequency of muonium, f_{LM} [Eq. (4.3)], in a static magnetic field rather than to induce a Zeeman transition with an rf magnetic field.

Experimental Method and Apparatus

The principle of the experiment was similar to the experiment on the depolarization of muons (Sec. 4) except that the muonium precession frequency f_{LM} of Eq. (4.3) rather than the free-muon precession frequency $f_{L\mu}$ of Eq. (4.1) was sought.[7,73] Figure 6 again shows the experimental arrangement. With the initial muon polarization in the positive z direction (direction of quantization) and with a weak magnetic field $\vec{H}$ in the x direction, muonium will be formed in states 1, 2, 3, and 4 (Fig. 1) with relative populations $\frac{1}{2}, \frac{1}{4}, 0$, and $\frac{1}{4}$, respectively [Eq. (3.11)]. Only in the occupied state 1 does muonium have a large magnetic moment [Eq. (4.2)]. This magnetic moment will precess about $\vec{H}$ in the yz plane with the Larmor frequency f_{LM}. Hence the number of positron counts observed in the 45 counter telescope as a function of time after the muons stop in the gas should be modulated with the frequency f_{LM} if polarized muonium is present. The experiment consisted in measuring the time distribution of decay positrons with respect to stopped muons, and then in analyzing the data for the frequency f_{LM} characteristic of muonium precession.

Muon Beam, Detectors, and Magnetic Field

The muon beam was discussed in Sec. 4. The scintillation counters were the same as discussed in Sec. 4.

The time interval between a stopped muon count $12\bar{3}$ and the subsequent positron count $45\bar{2}$ was measured[66] with a time-to-pulse height converter and a 100-channel pulse-height analyzer.[74] The fast coincidence circuits, modified from the circuit used in the depolarization experiment of Sec. 4, used IN34 germanium diodes to achieve a resolution time of a few nsec.[73] Following discriminators, a gating circuit was used so that only $12\bar{3}$ and $45\bar{2}$ pulses were analyzed, for which the time delay between $12\bar{3}$ and $45\bar{2}$ was between 0.2 and 2.0 μsec. Accidental counts were also measured by introducing an artificial delay of 5 μsec in the $12\bar{3}$ start pulse. Use of the lower limit of 0.2 μsec eliminated some background associated with pions and avoided the time interval region for which the measurement has a large fractional inaccuracy. The upper limit of 2.0 μsec was made equal to the muon mean life since, for longer time intervals, the fractional number of accidental counts increased. The time-to-pulse height converter was based on the charging of a condenser with a constant current for the time interval between the $12\bar{3}$ start pulse and the $34\bar{2}$ stop pulse and utilized the 6922 tube in the charging circuit. The linearity and stability of the time measurement were tested using a pulse generator as a source of start pulses and a radioactive source to produce random stop pulses; the system was also calibrated frequently during data-taking with the use of a crystal controlled time marker generator. These tests indicated that the system was accurate to about 1%.

Magnetic fields of about 4 G were used, which would result in 10 precession cycles during the 2-μsec observation time. The magnetic field was provided by the Helmholtz coils described in Sec. 4 and the field current was provided by a current-regulated supply.[75] The magnetic field was mapped with the use of an electron resonance spectrometer using diphenyl-picryl-hydrazyl (DPH) free radicals.[76] The total variation of the magnetic field over the region of the gas target was less than 2% and was caused principally by the fringing field of the synchrocyclotron magnet; this variation corresponds to a maximum phase difference in ten cycles of about 70° or a spread about the mean of ±35°.

Gas Purification

The target vessel has been described in Sec. 4. Argon gas with the impurity contents indicated in Table II was used at a pressure of 700 psi.

In order to purify[77] the Ar gas further and to avoid any increase of impurities due to outgassing from the target vessel, a gas recirculation and purification system was used as indicated in Fig. 8. The recirculation system comprised a ceramic lined inconel tube with about 150 g of titanium heated in a furnace to 500 °C, a heat exchanger

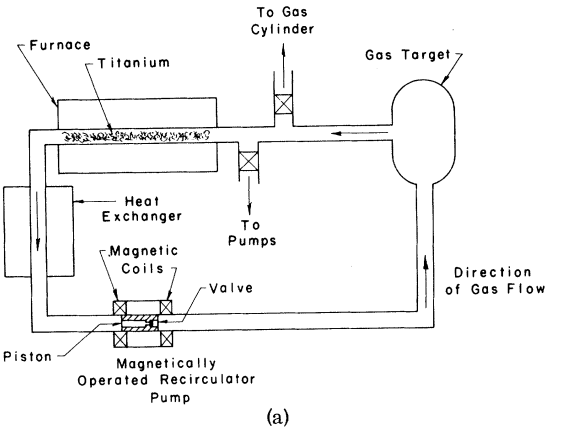

(a)

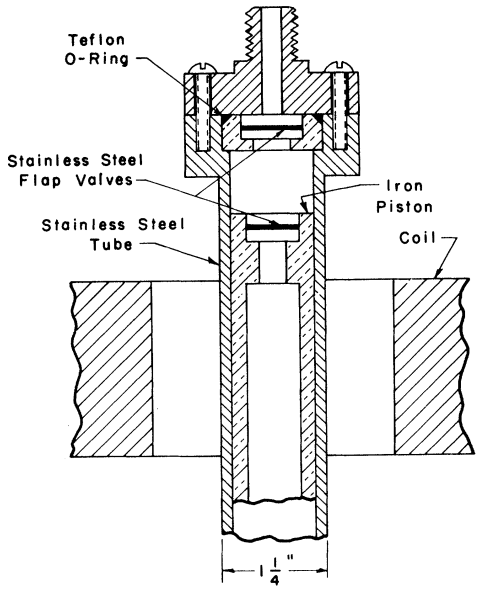

(b)

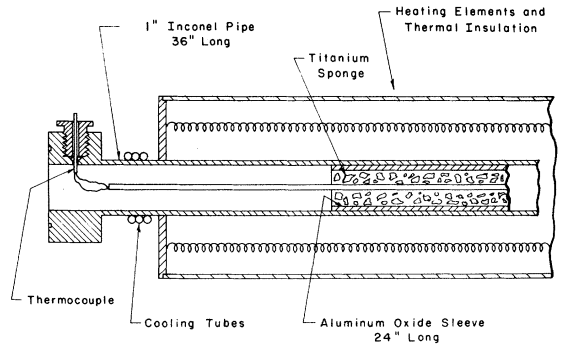

(c)

FIG. 8. (a) Schematic diagram of the gas recirculation and purification system used for the observation of the Larmor precession of muonium. (b) Detailed schematic diagram of the gas recirculation pump. (c) Detailed schematic diagram of the furnace.

and a pump. The homemade pump consisted of an iron piston within a stainless-steel tube and was operated by a solenoid at 1 cycle per 2 sec. A test of the purification system was made by filling the system with air to a pressure of 1 Torr and then observing the pressure decrease; after about 20 min the pressure dropped to about 10^{-2} Torr, thus indicating that all but the Ar component of the air had been taken up by the titanium.

Initially the target vessel and recirculation system were evacuated and outgassed by heating the titanium and flaming the target vessel until a pressure of about 2×10^{-6} Torr was attained. Then the system was filled with Ar to a pressure of 700 psi, and the purification system was operated for at least 24 h before data were taken. The pump was not operated during data-taking in order to avoid its effect on the magnetic field at the gas target.

Data and Data Analysis

Data were obtained in a period of about 200 h of synchrocyclotron operation which corresponded to about 5×10^7 $12\bar{3}$ stopped muon counts. For a particular value of the magnetic field H, data were accumulated of the 01 monitor counts, the $12\bar{3}$ stopped muon counts, the $45\bar{2}$ positron counts, the gated $45\bar{2}$ counts (events), pulse-height analyzer (PHA) counts corresponding to the distribution of time delays between events and $12\bar{3}$ counts, and finally accidental counts. The $12\bar{3}$ rate was typically 70 counts per sec. The $45\bar{2}$ rate was about one-fifth of the $12\bar{3}$ rate. The events rate was about 8×10^{-3} times the $12\bar{3}$ rate and hence some 4×10^5 PHA counts were accumulated. The accidental counting rate was one-tenth of the events rate. Data were obtained for values of H at 3.91, 4.34, 4.50, and 4.96 G. A typical set of PHA data is shown in Fig. 9.

In addition, in order to provide a check of our experiment, data were obtained with 4.34 and 4.50 G when pions rather than muons were stopped in the gas target, which was achieved by removing 4 in. of carbon absorber before counter 2. Decay muons from the stopped pions stopped in the gas target, but these muons were unpolarized due to the isotropic angular distribution of the muons from pion decay; hence no muonium precession is expected in this situation. Also, data were obtained when an aluminum target $3\times3\times1$ in. (the 1 in. thickness is along the muon beam direction) replaced the gas target and a field H of 94 G was applied. With this condition the 1.2 Mc/sec precession frequency of free polarized muons should be observed.

The time distribution data obtained from the PHA were assumed to be represented by

$$N(t)=N^1(t)+N^2(t)+N^3(t)+N^4(t)\ , \qquad (5.1a)$$

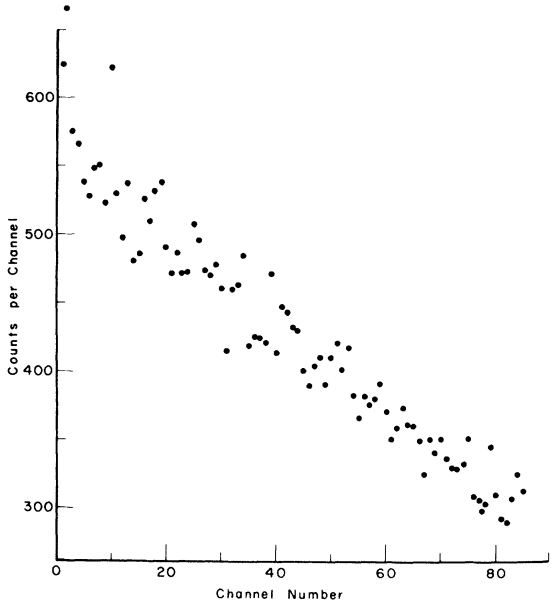

FIG. 9. A typical set of output PHA data, obtained with $H = 4.96$ G.

$$N^1(t) = C^1 e^{-(t_i + t_0)/\tau} \times \{1 + A^1 e^{-(t_i + t_0)/\tau'} \sin[2\pi f(t_i + t_0)]\}, \quad (5.1b)$$

$$N^2(t) = C^2 e^{-(t_i + t_0)/\tau} \times \{1 + A^2 \sin[2\pi f_{L\mu}(t_i + t_0)]\}, \quad (5.1c)$$

$$N^3 = C^3 e^{-(t_i + t_0)/\tau}, \quad (5.1d)$$

$$N^4(t) = C^4. \quad (5.1e)$$

The term $N^1(t)$ is associated with muonium in the $(F, M_F) = (1, 1)$ state. The quantities in Eq. (5.1b) have the following meanings: τ is the muon mean lifetime = 2.20 μsec; $C^1 = F_{M1} N_\mu d\Omega/(4\pi\tau)$; N_μ is the number of stopped muons (total number of $12\bar{3}$ counts); F_{M1} is the fraction of stopped muons forming muonium in state 1 (see Fig. 1); $d\Omega$ is the solid angle subtended by the positron telescope 45 at the gas target; $A^1 = SG' a_\mu$; S is a correction factor associated with the angular acceptance [Eq. (4.6)]; $G' = \sin(2\pi f_{LM}\Delta t)/(2\pi f_{LM}\Delta t)$, a correction factor associated with the PHA channel width Δt ($\Delta t \simeq 0.02$ μsec); $a_\mu = -\frac{1}{3}A \simeq +\frac{1}{3}$ [Eq. (2.9)]; τ' is a line-broadening parameter to be discussed later. The quantity f is the trial value for the precession frequency of the magnetic moment of muonium; t is the time interval between emission of positron and $12\bar{3}$ count; t_0 is the time interval between the time of $12\bar{3}$ count and the time of a subsequent positron emission which would register at the midtime of channel 5 of the PHA. t_i is the time interval between midtime of channel i and time t_0. Hence $t = t_0 + t_i$ is the time interval between a $12\bar{3}$ count and the time of a subsequent positron emission which would register at the midtime of channel i.

The term $N^2(t)$ is associated with polarized muons which have the Larmor precession frequency $f_{L\mu}$ [Eq. (4.1)]. C^2 "equals" $F_\mu N_\mu d\Omega/(4\pi\tau)$; F_μ is the fraction of stopped muons which precess as free polarized muons; A^2 "equals" $SG'' a_\mu$; $G'' = \sin(2\pi f_{L\mu}\Delta t)/(2\pi f_{L\mu}\Delta t)$.

The term $N^3(t)$ is associated with unpolarized muons. Muons in the muonium states $(F, M_F) = (1, 0)$ and $(0, 0)$ are essentially unpolarized. Free unpolarized muons or unpolarized muons bound in any atomic or molecular configuration will also contribute to $N^3(t)$. C^3 "equals" $F_3 N_\mu d\Omega/(4\pi\tau)$; F_3 is the fraction of stopped muons which are unpolarized.

The term $N^4(t)$ is associated with accidental counts. $N^4(t)$ "equals" C^4, in which C^4 is a constant.

A so-called line-broadening term $e^{-t/\tau'}$ has been introduced in the time distribution function $N^1(t)$ associated with muonium precession. Possible causes include depolarization and destruction of muonium in collisions, magnetic field inhomogeneities, and drifts in the electronics resulting, for example, in changes in t_0 or Δt. The correct form for the line-broadening term differs for these different causes. The term $e^{-t/\tau'}$ that has been used is correct only when depolarization of muonium in collisions is involved, where τ' is then the mean time between depolarizing collisions. However, our data are not sufficiently accurate statistically to allow us to distinguish the relative amounts of these various contributions to line broadening; hence we have represented the line broadening by the single term $e^{-t/\tau'}$ with the single parameter τ'.

The time distribution function $N(t)$ of Eq. (5.1a) which we fit to the observed data is considered to have the seven adjustable parameters $F_{M1}, F_\mu, F_3, C^4, t_0, \tau'$, and f. The parameter τ is taken equal to the mean lifetime of the free muon (2.20 μsec); with the instantaneous muon stopping rates in our experiment ($\sim 10^3$/sec) accidental coincidences between the 1.8-μsec delayed gate pulse generated by one stopped muon pulse $12\bar{3}$ and decay positrons from other stopped muons were very infrequent and their effect on the apparent muon lifetime was negligible.[66] Another effect that is sufficiently small for us to neglect is associated with muonium depolarizing collisions which actually convert muons from contributing to $N^1(t)$ to contributing to $N^3(t)$; the associated time dependence of the amplitudes of F_{M1} and F_3 is small and has been neglected. A clarification of the meaning of F_{M1} is useful. If the stopped muons are completely polarized, then F_{M1} is indeed

the fraction of the muons that form the muonium state 1; however, if the muons are only partially polarized, then F_{M1} should be interpreted as the difference between the fractions of the muons that form muonium in states 1 and 3.

A fit of the PHA data obtained at each magnetic field point H was made to the assumed time distribution function $N(t)$ of Eq. (5.1a) by the maximum likelihood method which reduces to the least-squares method, since the counts in the individual channels are distributed according to the Poisson distribution.[78,79] An IBM 650 computer was used for these computations. The procedure involved first fitting the data points x_i (counts in PHA channel i) by the function

$$N(t) - N^1(t) = N^2(t) + N^3(t) + N^4(t) \equiv n(t) \quad , \quad (5.2)$$

which varies only slowly with t since it does not contain the rapidly varying function $N^1(t)$. This fit determines to a rather good approximation the parameters t_0, F_μ, F_3, and C^4 since the contribution of the rapidly varying function $N^1(t)$ to the determination of the other slowly varying terms is small.

Using the function $n(t)$ so determined we computed the quantities

$$y_i = x_i - n(t_0 + t_i) \quad . \quad (5.3)$$

The y_i should be due principally to the rapidly oscillating term $N^1(t)$. Figure 10 shows a typical set of y_i values. A least-squares fit to the y_i was then made using the function

$$Y(t) = e^{-(t_i + t_0)/\tau} \times \{C + A^1 e^{-(t_i + t_0)/\tau'} \sin[2\pi f(t_i + t_0)]\} \quad , \quad (5.4)$$

in which C, A^1, τ', and f are the adjustable parameters. The term with the parameter C is introduced to represent a possible small residual, slowly varying background associated with the y_i values. The χ^2 test was applied to the fits and some correlated errors or off-diagonal elements in the error matrix were calculated.

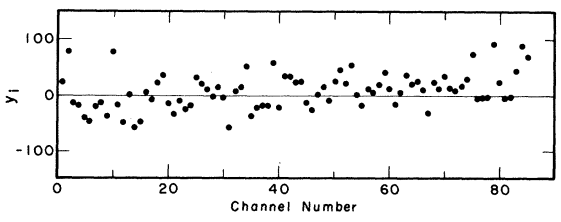

FIG. 10. A typical set of values y_i versus PHA number, obtained with $H = 4.96$ G.

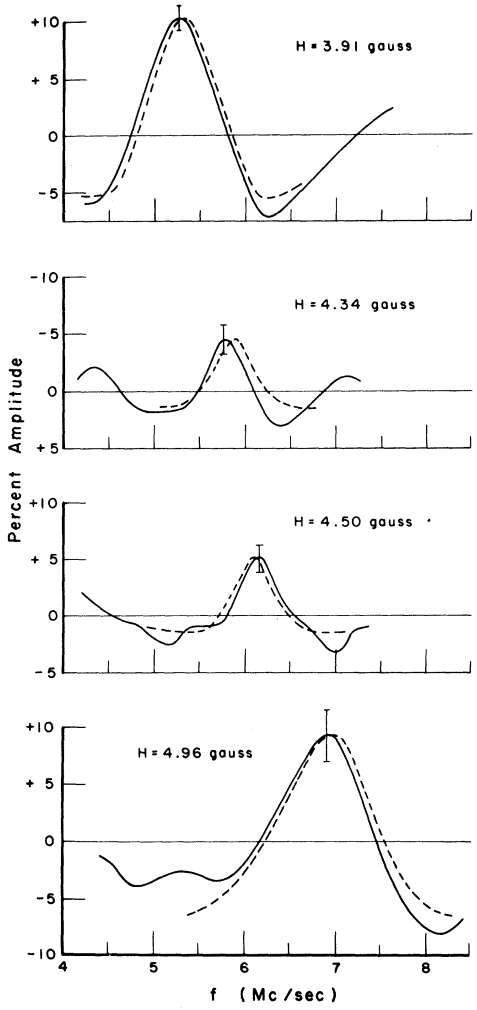

FIG. 11. Frequency analysis illustrating the precession of positive muons stopped in aluminum with $H = 94$ G. The percent amplitude of a frequency component, r, is plotted versus frequency.

Figure 11 shows the result of the analysis of the data obtained when muons were stopped in an aluminum target in a magnetic field H of 94 G. For this case the term $N^1(t)$ in Eq. (5.1a) can be omitted and the frequency parameter f replaces $f_{L\mu}$ in the analysis. The ordinate is the ratio of amplitudes, $r = A^2C^2/(C^2 + C^3 + C^4)$, expressed in percent. It has its maximum value of 27% at $f = 1.27$ Mc/sec, which agrees with the expected Larmor precession frequency of a free muon of 1.27 Mc/sec [Eq. (4.1)]. The value $R = 0.27$ is also close to the maximum value to be expected for completely polarized free muons. The linewidth is due principally to the limited gate time of 1.8 μsec during which the precession is observed. This result provides a check of our analysis procedure and of the operation of our equip-

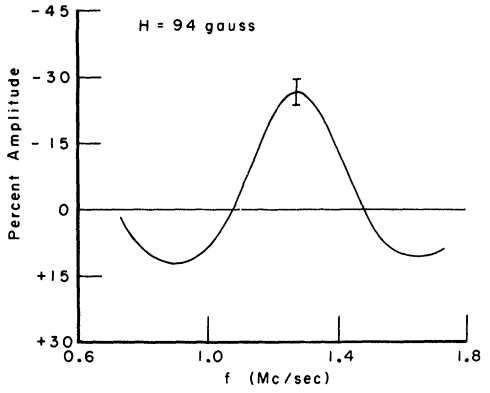

FIG. 12. Frequency analysis, illustrating the precession of muonium when polarized muons are stopped in argon gas for several magnetic field values H. The percent amplitude of a frequency component, r, is plotted versus frequency.

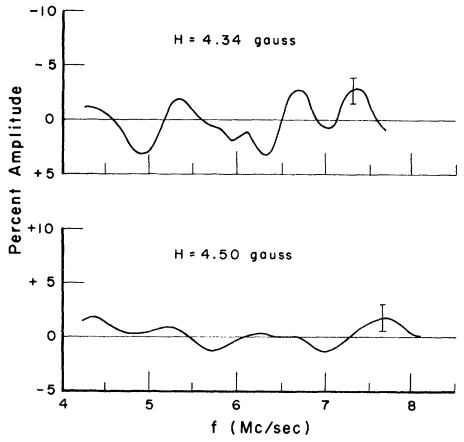

FIG. 13. (a) Values of χ^2 versus frequency f for various values of t_0, obtained from the least-squares fit to the data with polarized muons and $H=4.34$ G (t_0 in μsec). (b) Values of χ^2 and peak amplitude F_{M1} versus the parameter τ', obtained from the least-squares fit to the data with polarized muons and $H=4.34$ G.

ment, particularly of the electronics system.

Figure 12 shows the results of the data analysis for the cases in which polarized muons were stopped in the gas target with $H=3.91$, 4.34, 4.50, and 4.96 G. The ratio $r=C^1A^1/(C^1+C^2+C^3+C^4)$ is plotted as a function of f. The meaning of r is the ratio of PHA counts associated with the muonium precession term to the PHA counts associated with all the other terms in Eq. (5.1a). The solid curves are obtained from the data analysis, and the error bar is a typical 1 standard deviation error. Each dashed curve is a theoretical line shape computed from the distribution function

$$Y^0(t)=C^0e^{-t_i/\tau}\times e^{-t_i/\tau'}\sin 2\pi f_{LM}(t_i+t_0)\ , \qquad (5.5)$$

in which C^0 is a normalization constant. Its central maximum occurs at the muonium precession frequency f_{LM} predicted from Eq. (4.3) for the measured value of H. The theoretical curve was computed with the values of τ' and t_0 determined from the data analysis. The normalization constant C^0 was chosen so that the peak amplitude of the theoretical curve equals the peak amplitude of the solid curve. The dashed curve is essentially the Fourier spectrum of $Y^0(t)$. Its width is determined by the gate interval of 1.8 μsec and by τ'.

Resonances are clearly observed in all four cases in Fig. 12 at the predicted frequencies, and the amplitudes of the resonances are 4, 4, 5, and 4 standard deviations from zero, respectively. The amplitudes of the resonances vary between 5 and 10%. Possible causes of variation include gas impurities, magnetic field inhomogeneities, and instabilities in the electronics. We note that the larger values of the amplitudes occur with the smaller values of the line-broadening parameter τ'. Table IV provides data on the individual fits, including χ^2 values. Figure 13(a) gives information on correlated errors involving the fitting parameters t_0 and f, and Fig. 13(b) shows plots of the

TABLE IV. Results of analysis of data on Larmor precession of muonium.[a]

	$H=3.91$ G	$H=4.34$ G	$H=4.50$ G	$H=4.96$ G
t_0(μsec)	0.300 ± 0.07	0.335 ± 0.010	0.300 ± 0.009	0.273 ± 0.011
ΔH(%)	1.0 to 1.6	0.3 to 1.6	1.6	2
τ' (μsec)	0.5 ±1.0	1.5 ±1.0	1.4 ±1.0	0.3 ±1.0
F_μ	0.6 ±0.1	0.6 ±0.1	0.6 ±0.1	•••
$2F_{M1}$(%)[b]	300 ±100	90 ± 40	100 ±50	•••
f(Mc/sec)	5.25 ± 0.16 (±2.9%)	5.82 ± 0.20 (±3.3%)	6.17 ± 0.23 (±3.6%)	6.96 ± 0.28 (±4.0%)
χ^2	86 ± 13	76 ± 13	76 ± 13	80 ± 13

[a]The data for each field value H have 87 degrees of freedom.

[b]$F_3 \simeq F_{M1}$.

values of F_{M1} and χ^2 versus τ', both for the case with $H=4.34$ G. Agreement between the observed data and the fitted function $N(t)$ is satisfactory in all cases. Agreement between the experimental values of the resonant frequencies and the predicted values is within 4% as 1 standard deviation in all cases. Analyses of the data were made using functions other than $e^{-ti/\tau'}$ to represent line broadening; however, the statistical quality of the data was not sufficiently good to distinguish the fits to the different functions.

Figure 14 shows the results of analysis of data obtained when pions were stopped in the gas target. The data for $H=4.50$ G were taken immediately before the data for $H=4.50$ G shown in Fig. 12 and those for $H=4.34$ G immediately after the data for $H=4.34$ G shown in Fig. 12. No muonium resonances are observed in Fig. 14, as expected.

Analysis of the data can be made to determine a rough value for the fraction of the muons stopping in the gas that form muonium in state 1. This determination depends, of course, on the amplitude of the resonance signal and on the fraction of the muons stopping in the walls of the target. We have noted that the amplitude of the resonance signal varies between 5 and 10% for different cases. From the data of Sec. 4 we know that about one-half the muons stop in the target walls. Only one-half the muons with 100% polarization which form muonium will do so in state 1, whose precession we observe. Hence an amplitude of 8% for the resonance signal implies 100% muonium formation by the muons stopped in the gas.

Results and Discussion

Our data indicate beyond any reasonable doubt that polarized muonium is formed and that its polarization is retained when polarized muons are stopped in pure argon gas.[7] The fraction of the muons stopping in the gas that form muonium is only roughly determined; it appears to be close to 100% and is at least greater than 50%. This large value for the muonium formation probability is consistent with the discussion in Sec. 3.

The observation of a precession signal for polarized muonium at the characteristic Larmor precession frequency given by Eq. (4.3) also constitutes a rigorous proof[60,80] that the spin of the muon is $\frac{1}{2}$. Our precession experiment constitutes a measurement of the magnetic moment of muonium in state 1 at weak magnetic field [Eq. (2.6)] or equivalently of the g factor g_F which characterizes the Zeeman effect. The usual expression for the g_F value is[28]

$$\mu_1 = g_F \mu_B^e ,$$

where

$$g_F = \frac{F(F+1)+J(J+1)-I_\mu(I_\mu+1)}{2F(F+1)} g_J + \frac{F(F+1)+I_\mu(I_\mu+1)-J(J+1)}{2F(F+1)} \frac{m_e}{m_\mu} g_\mu . \quad (5.6)$$

Since we are concerned with the state for which $F=J+I_\mu=I_\mu+\frac{1}{2}$ and since the second term is small, a useful approximate expression is

$$g_F \simeq g_J/(2I_\mu+1) . \quad (5.6')$$

The close agreement of the observed magnetic moment with the value $\frac{1}{2} g_J \mu_B^e$ provides a proof that $I_\mu=\frac{1}{2}$. This method of determination of the

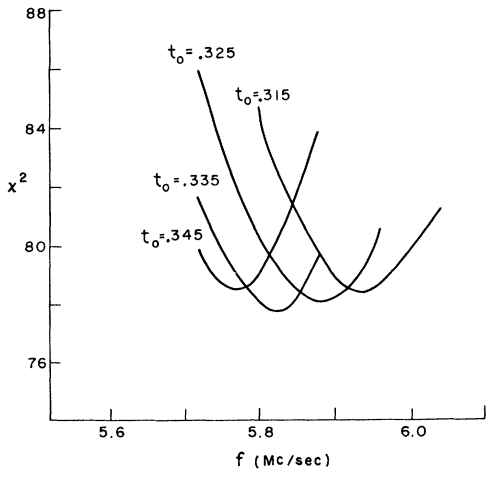

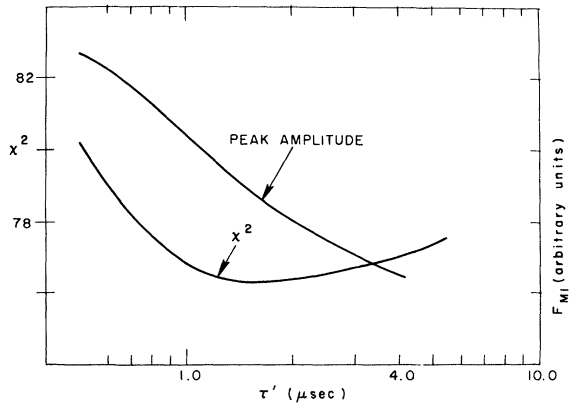

FIG. 14. Frequency analysis of data obtained when pions are stopped in argon gas for several magnetic field values H. The percent amplitude of a frequency component, r, is plotted versus frequency.

muon spin is essentially the same as the method of determining nuclear spins based on the measurement of the atomic Zeeman effect.[28,81]

6. DETERMINATION OF hfs INTERVAL THROUGH A STATIC MAGNETIC FIELD MEASUREMENT

In view of the abundant formation of polarized muonium in pure argon discussed in Sec. 5, an experiment was undertaken to obtain a rough measurement of $\Delta\nu$ and to confirm further the expected behavior of muonium by observation of the effect of a static magnetic field.[8]

The principle of the experiment can be understood with reference to Eq. (3.12), which gives the polarization of the muons that form muonium as a function of the static magnetic field $\vec{H}$. The field $\vec{H}$ is in the positive z direction, which is also the direction of polarization of the incident muons. If P is measured as a function of H and the quantities $g_J\mu_B{}^e/h$ and $g_\mu\mu_B{}^\mu/h$ are given their known values[25,82] [see Eq. (2.2)], then the measured $P(H)$ can be used to determine a value for $\Delta\nu$. Measurement of the muon polarization relies on the asymmetry of the decay positron angular distribution as given by Eq. (2.9)

$$N(\theta) \propto 1 + \tfrac{1}{3} P \cos\theta. \qquad (2.9)$$

Experimental Method and Apparatus

The experimental arrangement is shown in Fig. 15.[8,83] The longitudinal magnetic field $\vec{H}$ in the positive z direction is provided by a solenoid magnet. Muons stopped in the argon gas target were indicated by $12\bar{3}$ coincident counts, and decay positrons were observed in the negative z direction as $34\bar{2}$ coincident counts in the time interval from 0.2–3.2 μsec after a stopped muon count. Measurements were taken as a function of H. In order to account for the effect of the magnetic field H on positron trajectories and hence on the probabilities for decay positrons to reach the positron telescope, measurements were also made with a dummy target.

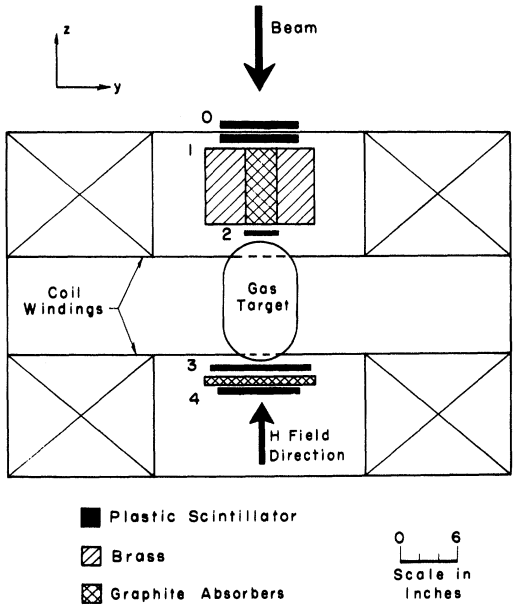

FIG. 15. Schematic diagram of the experimental arrangement for measurement of $\Delta\nu$ with the use of a static magnetic field.

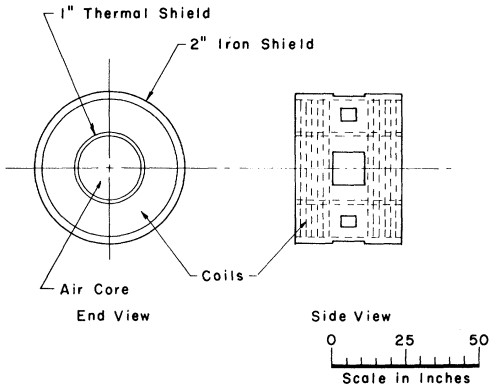

FIG. 16. Schematic drawing of solenoid magnet.

The muon beam was the same as that discussed in Secs. 4 and 5. The scintillation counters 0, 1, 2, and 3 were the same as those used in the experiment discussed in Sec. 5. Scintillation counter 4 was an 8-in.-square plastic scintillator with its Lucite light pipe lying along the z direction. Tests showed that there was no change in any counter's output voltage as H was varied 0–5800 G, and the counter voltages were well plateaued in the magnetic field. The range curves were the same with and without the magnetic field. The electronics circuitry and logic were essentially the same as for the muon depolarization experiment (Sec. 4). A gate pulse having a width of 3.0 μsec and delayed by 0.2 μsec was triggered by a $12\bar{3}$ coincidence or stopped muon pulse, and a coincidence of a $34\bar{2}$ positron pulse with the gate produces a positron event pulse. Accidental counts were obtained when the gate pulse was delayed by an additional 4 μsec. The beam intensity was monitored by the 01 counts.

The magnetic field H was provided by an air-core solenoid with two lengths of windings, as indicated in Fig. 16. The diameter of the air core was 21 in. and the over-all length of the magnet was 36 in. A 2-in.-thick iron shield extended the total length of the magnet outside the coils except for an opening at the middle of the magnet between the two windings. The magnet was powered from a 300-kW motor generator whose output was fil-

tered so that the peak ripple in the output current was less than 1%. The magnetic field was stabilized by voltage feedback to the motor generator. The current was monitored by the voltage reading across a shunt and the magnetic field was measured with an NMR probe.

The gas target was the same one described in Secs. 4 and 5, including the recirculation and purification system. Pure argon at a pressure of 55 atm was used. The dummy target described in Sec. 4 was also used.

Data and Data Analysis

Data were obtained of 01, $12\bar{3}$, $34\bar{2}$, events and accidental counts for each of the four conditions discussed in Sec. 4 at each magnetic field H used. Seven values of H between 200 and 6000 G were used. Approximately 10 000 event pulses were accumulated for each magnetic field value for both the gas target and the dummy target.

Analysis of the data to obtain the polarization $P(H)$ of the muons that form muonium in a magnetic field H is based on the equations

$$N^1(H) = N_g(H)(1 - \tfrac{1}{3}SP)/(1 - \tfrac{1}{3}S) + N_w(H) + N_2(H) \quad , \tag{6.1a}$$

$$N^2(H) = N_{\mathrm{Al}}(H) + N_w(H) + N_2(H) \quad , \tag{6.1b}$$

$$N^3(H) = N_{\mathrm{Al}}(H) + N_2(H) \quad , \tag{6.1c}$$

$$N^4(H) = N_2(H) \quad , \tag{6.1d}$$

in which $N^1(H), N^2(H), N^3(H)$, and $N^4(H)$ are the events counts with a magnetic field H for a fixed number N_0 of monitor counts [refer to definitions of Eq. (4.6)], corresponding to the four conditions of Sec. 4. The quantities $N_{\mathrm{Al}}(H), N_w(H)$, and $N_2(H)$ are the events counts due to the aluminum, the walls, and counter 2, respectively. The quantity $N_g(H)(1 - \frac{1}{3}SP)/(1 - \frac{1}{3}S)$ is the events counts due to the gas, where the factor $(1 - \frac{1}{3}SP)/(1 - \frac{1}{3}S)$ accounts for the polarization of muons that form muonium in the field H and for the associated position decay asymmetry. [The quantity S is a correction factor associated with angular acceptance which was defined for Eq. (4.6).] The above equations apply, of course, when $H = 0$.

In order to obtain a useful result from these equations we define the ratios

$$R_{\mathrm{Al},w} = \frac{N^2(H) - N^4(H)}{N^2(0) - N^4(0)} = \frac{N_{\mathrm{Al}}(H) + N_w(H)}{N_{\mathrm{Al}}(0) + N_w(0)} , \tag{6.2a}$$

$$R_{g,w} = \frac{N^1(H) - N^4(H)}{N^1(0) - N^4(0)} = \frac{N_g(H)[h(H)+1] + N_w(H)}{N_g(0)[h(0)+1] + N_w(0)} , \tag{6.2b}$$

$$R = \frac{R_{\mathrm{Al},w}}{R_{g,w}} = \frac{1 + h(0)g(0)}{1 + h(H)g(H)} , \tag{6.2c}$$

in which $h(H) \equiv (1 - \frac{1}{3}SP)/(1 - \frac{1}{3}S) - 1$; $h(0) \equiv (1 - \frac{1}{6}S)/(1 - \frac{1}{3}S) - 1$; $g(H) \equiv N_{\mathrm{Al}}(H)/[N_{\mathrm{Al}}(H) + N_w(H)]$. In the derivation of Eq. (6.2c) from Eqs. (6.1) it is assumed that $N_{\mathrm{Al}}(H) = N_g(H)$ (the argon gas pressure is chosen so that this condition should apply), and that the polarization of the muons stopped in the aluminum and the walls has the polarization value of the incoming muon beam (assumed to be 1.0) independent of the value of H. The quantity $g(H)$ is the fraction of the muons that stop in the gas. The quantity S has the value 0.955. The quantity R can be regarded as a ratio normalized to the dummy target data and to zero value for the magnetic field H. Actually the lowest value of H used was 200 G, in order to assure that no depolarization of muonium occurred due to nonadiabatic transitions associated with a near-zero magnetic field condition or due to magnetic interactions in muonium collisions. For $H = 200$ G the value of P is 0.508 and hence very close to the value $P = 0.500$ for $H = 0$.

The experimental values for $R_{Al,w}, R_{g,w}, g$, and R are given in Table V. To obtain these val-

TABLE V. Experimental data from static magnetic field measurements.

H(G)	$R_{\mathrm{Al},w}$	$R_{g,w}$	g	R
Run (1)				
200	1.000	1.000	0.38 ± 0.01	1.00 ± 0.02
1500	1.012 ± 0.02	1.015 ± 0.02	0.38 ± 0.01	1.00 ± 0.03
2600	1.073 ± 0.02	1.021 ± 0.02	0.35 ± 0.01	1.05 ± 0.03
6000	1.234 ± 0.02	1.129 ± 0.02	0.35 ± 0.01	1.09 ± 0.03
Run (2)				
200	1.000	1.000	0.42 ± 0.02	1.00 ± 0.02
1170	1.014 ± 0.01	0.982 ± 0.01	0.42 ± 0.02	1.033 ± 0.02
2650	1.066 ± 0.01	1.019 ± 0.01	0.44 ± 0.02	1.047 ± 0.02
5520	1.214 ± 0.01	1.158 ± 0.01	0.42 ± 0.02	1.049 ± 0.02

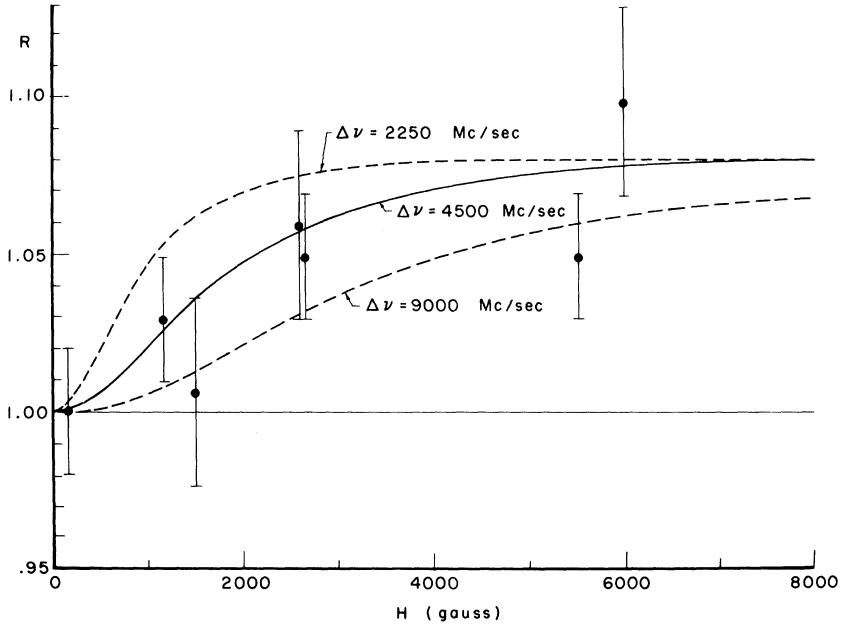

FIG. 17. Experimental data and theoretical curves for the quantity R versus the static magnetic field H. The experimental value for R is obtained from Eq. (6.2c), and the theoretical value is calculated from Eq. (3.12).

ues the N values were corrected for about a 5% accidental rate, and the indicated errors are 1 standard deviation. The data were obtained in two experimental runs.

Figure 17 shows the experimental values for the ratio R as a function of magnetic field H. All the data have been normalized to the value $g = 0.4$. Theoretical curves for $R(H)$ are shown for different assumed values of the hfs interval $\Delta\nu$. These theoretical curves are obtained under the assumption that all muons stopping in the argon gas form muonium.

Clearly, the best agreement is obtained with the theoretical curve having $\Delta\nu = 4500$ Mc/sec. Indeed a least-squares fit of the experimental data to the theoretical curve gives:

$$\Delta\nu = 5500^{+2900}_{-1500}\ \text{Mc/sec}\ , \qquad (6.3)$$

where 1 standard deviation statistical errors are indicated. The principal error in the determination of $\Delta\nu$ in this experiment arises from the statistical counting error; a relatively smaller systematic error is present due to uncertainty in the determination of the fraction of muons g that stop in the gas (see Sec. 4).

The conclusion of this experiment with a static magnetic field is that there is qualitative agreement of the measured value of the hfs interval with the theoretical value. The accuracy of the measurement of $\Delta\nu$ is about 50%.

APPENDIX A: THEORETICAL CALCULATION OF MUONIUM FORMATION BY CHARGE CAPTURE FROM HELIUM

The simplest charge-capture reaction resulting in ground-state muonium formation that is relevant to our experiment is the reaction

$$\mu^+ + \text{He} \rightarrow \text{M} + \text{He}^+ . \qquad (A1)$$

The charge-capture reaction involving H is simpler because only a single electron is involved, but at present it does not seem accessible to experimental study and it contains the special feature of a near-resonance charge transfer which is not generally involved for other atoms.

A summary of our theoretical calculations, whose results are displayed in Fig. 3, is given below. The calculations employ three different approximations for three different kinetic-energy regions of the incident muon: (1) the low-energy region where the incident muon velocity v_μ is small compared to αc, a characteristic electron velocity in helium, (2) the intermediate-energy region where $v_\mu \simeq \alpha c$, (3) the high-energy region where $v_\mu \gg 2\alpha c$.

For the low-energy region the perturbed stationary state (PSS) method[35] was employed. The formulation used by Massey and Smith[84] to calculate charge capture by H^+ from He at low energies was followed.[85] Also the same simple wave functions were employed except that a smoother variation of the initial-state wave function with their parameter Z was taken. The integrations were done using elliptic coordinates. Values for the capture cross section were calculated for the muon kinetic energy E_μ up to 50 eV. Although the threshold energy is 11.0 eV, the capture cross section is very small below the so-called "activation energy" at about 40 eV. Above this energy the cross section rises rapidly.[86]

For the intermediate-energy range an impact-

parameter method, in a two-state moving-atom approximation,[35] was used. The formulation used by Green, Stanley, and Chiang[87] was taken and values for the capture cross section were calculated for E_μ between 50 eV and 9 keV.

For the high-energy range the Born approximation[35] was used. The calculation by Mapleton[88] was modified for our case [Eq. (A1)], and values were calculated for $E_\mu > 9$ keV.

APPENDIX B: THEORETICAL CALCULATION OF DISTRIBUTION IN FINAL hfs STATES IN MUONIUM FORMATION

For a theoretical discussion of the distribution of muonium in the four hfs states of the ground state $1^2S_{1/2}$ resulting from muonium formation in a charge-capture reaction, it is sufficient to take the Hamiltonian

$$\mathcal{H} = \mathcal{H}_e + \mathcal{H}_m \ , \tag{B1}$$

in which $\mathcal{H}_e$ is a nonrelativistic Schrödinger Hamiltonian including the kinetic-energy and Coulomb interaction terms and $\mathcal{H}_m$ is the Hamiltonian term of Eq. (2.2) which includes the magnetic interaction terms for muonium.

Two different viewpoints can be taken. In the first,[89] we treat the charge-capture reaction as a single process involving the entire Hamiltonian $\mathcal{H}$ and take the final states of the charge-capture reaction to be eigenstates of the total Hamiltonian $\mathcal{H}$. It is easiest to apply this viewpoint in the Born approximation for the charge-capture reaction.[35] The initial and final eigenstates Ψ_i and Ψ_f are given in the Pauli approximation as products of spatial and spin eigenfunctions

$$\Psi_{i(f)} = \Psi_{i(f)}(\vec{\mathbf{r}})\chi_{i(f)} \ , \tag{B2}$$

in which $\vec{\mathbf{r}}$ represents the spatial coordinates of all the particles and χ is a spin eigenfunction for the muon and one electron, as given in Eq. (2.4). The term in the Hamiltonian responsible for the charge-capture reaction is the term $\mathcal{H}_e$, and in the Born approximation only a matrix element of a portion of $\mathcal{H}_e$ between the initial and final states is involved. In this matrix element, the projection of the initial spin state on the final spin state appears, and hence the results given in Eq. (3.11) follow. The result of Eq. (3.12) for the polarization of the muons forming muonium is then obtained from Eq. (3.11) by taking the average of the muon polarization over the four muonium states, weighted according to their formation probabilities.

With other approximations for treating the charge-capture reaction such as are discussed in Appendix A for the reaction

$$\mu^+ + \mathrm{He} \rightarrow M + \mathrm{He}^+ \ ,$$

where again a separability of the wave function into a space part and a spin part is valid and the term $\mathcal{H}_e$ is responsible for the reaction, the results of Eq. (3.11) again apply.

In the second viewpoint[60] we consider the charge-capture reaction as a two-step process; in the first step we ignore the Hamiltonian term $\mathcal{H}_m$, and then in the second step we consider the effect of $\mathcal{H}_m$ on the final eigenstates. This viewpoint is useful because the electric charge-capture reaction without any change in the spin directions of particles takes place in a time very short compared to the time required ($\sim 1/\Delta\nu$) for the magnetic interaction term $\mathcal{H}_m$ to produce appreciable reorientation of the spins.

From this viewpoint, if we consider that incident muons are in the initial spin state α_μ in a longitudinal magnetic field $\vec{\mathbf{H}}$ in the z direction and that the atomic electrons have no net polarization, then as a result of the electric charge-capture reaction the following two muonium spin states are formed, each with probability $\frac{1}{2}$:

$$\begin{aligned} \chi_A &= \alpha_\mu \alpha_e \ , \\ \chi_B &= \alpha_\mu \beta_e \ . \end{aligned} \tag{B3}$$

Since the state χ_A is a spin eigenstate of muonium, $\chi_A = \chi_{1,1}$ [Eq. (2.4)], it is an appropriate spin part of a final eigenstate of the total Hamiltonian $\mathcal{H}$, and the Hamiltonian term $\mathcal{H}_m$ leaves this spin eigenfunction unchanged. On the other hand, the spin function χ_B is not an eigenstate of $\mathcal{H}_m$, and hence χ_B is only the spin function at the time $t = 0$ of muonium formation. The correct time-dependent spin function $\chi_B(t)$ is

$$\begin{aligned} \chi_B(t) = {} & C_1 \chi_{1,0}(H) e^{-iW_{1,0}t/\hbar} \\ & + C_2 \chi_{0,0}(H) e^{-iW_{0,0}t/\hbar} \ , \end{aligned} \tag{B4}$$

in which $C_1^2 + C_2^2 = 1$ (B5)

is a normalization condition,

and $cC_1 - sC_2 = 0$ (B6)

is a condition required to satisfy the initial condition

$$\chi_B(0) = \alpha_\mu \beta_e \ .$$

These equations imply

$$C_1 = s \quad \text{and} \quad C_2 = c \ . \tag{B7}$$

The quantities are defined in Eqs. (2.1) through (2.5). Hence the muon polarization $P_B(t)$ in this state is given by

$$P_B(t) = \frac{s^2/c^2 + c^2/s^2 - 2 + 4\cos(\Delta W t/\hbar)}{c^2/s^2 + s^2/c^2 + 2} . \quad \text{(B8)}$$

The time average of Eq. (B8) gives the average muon polarization in muonium states 2 and 4.

Equations (3.11), (3.12), and (B8) were obtained for the initial condition $\alpha_\mu = 1$. These equations are easily generalized to an arbitrary initial muon polarization.

---

*Research supported in part by the U.S. Air Force Office of Scientific Research (at Yale University) and by the U.S. Office of Naval Research (at Columbia University).

†Present address: University of California, Davis, Calif.

‡Present address: University of Virginia, Charlottesville, Va.

§Present address: University of Wisconsin, Madison, Wis.

[1]M. Gell-Mann, Rev. Mod. Phys. 31, 834 (1959).

[2]G. Feinberg and L. M. Lederman, Ann. Rev. Nucl. Sci. 13, 431 (1963).

[3]R. L. Garwin, L. M. Lederman, and M. Weinrich, Phys. Rev. 105, 1415 (1957).

[4]J. I. Friedman and V. L. Telegdi, Phys. Rev. 105, 1681 (1957).

[5]V. W. Hughes, Bull. Am. Phys. Soc. 2, 205 (1957).

[6]V. W. Hughes, A. Lurio, D. P. Malone, L. Lederman, and M. Weinrich, Bull. Am. Phys. Soc. 3, 51 (1958); D. McColm, V. W. Hughes, D. P. Malone, L. Lederman, and A. Lurio, *ibid.* 3, 229 (1958).

[7]V. W. Hughes, D. W. McColm, K. Ziock, and R. Prepost, Phys. Rev. Letters 5, 63 (1960).

[8]R. Prepost, V. W. Hughes, and K. Ziock, Phys. Rev. Letters 6, 19 (1961).

[9]V. W. Hughes, Ann. Rev. Nucl. Sci. 16, 445 (1966).

[10]V. W. Hughes, in Proceedings of the First International Conference on Atomic Physics, edited by V. W. Hughes, B. Bederson, V. W. Cohen, and F. J. Pichanick (Plenum Press, Inc. New York, 1969), p. 15.

[11]W. K. H. Panofsky, in Proceedings of the Fourteenth International Conference on High-Energy Physics (CERN, Geneva, 1968), p. 23.

[12]G. Källen, Handbuch der Physik, edited by S. Flügge (Springer-Verlag, Berlin, 1958), Vol. 5/1, p. 169.

[13]H. A. Bethe and E. E. Salpeter, Encyclopedia of Physics, edited by S. Flügge (Springer-Verlag, Berlin, 1957), Vol. 35/1, p. 88.

[14]K. Ziock, V. W. Hughes, R. Prepost, J. Bailey, and W. Cleland, Phys. Rev. Letters 8, 103 (1962).

[15]W. E. Cleland, J. M. Bailey, M. Eckhause, V. W. Hughes, R. M. Mobley, R. Prepost, and J. E. Rothberg, Phys. Rev. Letters 13, 202 (1964).

[16]P. A. Thompson, J. J. Amato, P. Crane, V. W. Hughes, R. M. Mobley, G. zu Putlitz, and J. E. Rothberg, Phys. Rev. Letters 22, 163 (1969).

[17]R. M. Mobley, J. M. Bailey, W. E. Cleland, V. W. Hughes, and J. E. Rothberg, in Proceedings of the Fourth International Conference on the Physics of Electronic and Atomic Collisions, Quebec, 1965, edited by L. Kerwin and W. Fite (Science Bookcrafters, Hastings-on-Hudson, New York, 1965), p. 194.

[18]R. M. Mobley, J. M. Bailey, W. E. Cleland, V. W. Hughes, and J. E. Rothberg, J. Chem. Phys. 44, 4354 (1966).

[19]R. M. Mobley, J. J. Amato, V. W. Hughes, J. E. Rothberg, and P. A. Thompson, J. Chem. Phys. 47, 3074 (1967).

[20]J. J. Amato, P. Crane, V. W. Hughes, D. L. Morgan, Jr., J. E. Rothberg, and P. A. Thompson, Phys. Rev. Letters 21, 1709 (1968); 21, 1786 (1968).

[21]V. G. Firsov, Zh. Eksperim. i Teor. Fiz. 48, 1179 (1965) [English transl.: Soviet Phys. – JETP 21, 786 (1965)].

[22]A. I. Babaev, M. Ya. Balats, G. G. Myasishcheva, Yu. V. Obukhov, V. S. Roganov, and V. G. Firsov, Zh. Eksperim. i Teor. Fiz. 50, 877 (1966) [English transl.: Soviet Phys. – JETP 23, 583 (1966)].

[23]G. G. Myasishcheva, Yu. V. Obukhov, V. S. Roganov, and V. G. Firsov, Zh. Eksperim. i Teor. Fiz. 53, 451 (1967) [English transl.: Soviet Phys. – JETP 26, 298 (1968)].

[24]The most recent and accurate value for the ratio m_μ/m_e is given in Ref. 17; however, the value given above is sufficiently accurate for the present paper.

[25]E. R. Cohen and J. W. M. DuMond, Rev. Mod. Phys. 37, 537 (1965).

[26]E. Fermi, Z. Physik 60, 320 (1930).

[27]G. Breit and I. I. Rabi, Phys. Rev. 38, 2082 (1931).

[28]P. Kusch and V. W. Hughes, Encyclopedia of Physics, edited by S. Flügge (Springer-Verlag, Berlin, 1959), Vol. 37/1, p. 1.

[29]T. D. Lee and C. S. Wu, Ann. Rev. Nucl. Sci. 15, 381 (1965).

[30]N. Barash-Schmidt, A. Barbaro-Galtieri, L. R. Price, A. H. Rosenfeld, P. Söding, C. G. Wohl, M. Roos, and G. Conforto, Rev. Mod. Phys. 41, 109 (1969).

[31]B. Pontecorvo, Zh. Eksperim. i Teor. Fiz. 33, 549 (1957) [English transl.: Soviet Phys. – JETP 6, 429 (1958)].

[32]C. K. Jen, S. N. Foner, E. L. Cochran, and V. A. Bowers, Phys. Rev. 112, 1169 (1958).

[33]F. M. Pipkin and R. H. Lambert, Phys. Rev. 127, 787 (1962).

[34]S. K. Allison, Rev. Mod. Phys. 30, 1137 (1958).

[35]N. F. Mott and H. S. W. Massey, The Theory of Atomic Collisions (Clarendon Press, Oxford, 1965), 3rd ed.

[36]D. R. Bates, in Atomic and Molecular Processes, edited by D. R. Bates (Academic Press Inc., New York, 1962), p. 550.

[37]J. B. Hasted, in Atomic and Molecular Processes,

edited by D. R. Bates (Academic Press Inc., New York, 1962), p. 696.

[38]J. B. Hasted, in Advances in Electronics and Electron Physics, edited by L. Marton (Academic Press Inc., New York, 1960), Vol. XIII, p. 1.

[39]J. B. H. Stedeford and J. B. Hasted, Proc. Roy. Soc. London A227, 466 (1954).

[40]P. M. Stier and C. F. Barnett, Phys. Rev. 103, 896 (1956).

[41]R. N. Il'in, V. V. Afrosimov, and N. V. Fedorenko, Zh. Eksperim. i Teor. Fiz. 36, 41 (1959) [English transl.: Soviet Phys. – JETP 9, 29 (1959)].

[42]S. K. Allison and M. Garcia-Munoz, in Atomic and Molecular Processes, edited by D. R. Bates (Academic Press Inc., New York, 1962), p. 721.

[43]E. W. McDaniel, Collision Phenomena in Ionized Gases (John Wiley & Sons, Inc., New York, 1964).

[44]H. S. W. Massey and E. H. S. Burhop, Electronic and Ionic Impact Phenomena (Clarendon Press, Oxford, 1969), 2nd ed.

[45]V. W. Hughes, Phys. Rev. 108, 1106 (1957).

[46]C. F. Giese, Advan. Chem. Phys. 10, 247 (1966).

[47]P. M. Stier, C. F. Barnett, and G. E. Evans, Phys. Rev. 96, 973 (1954).

[48]E. A. Mason and J. T. Vanderslice, Atomic and Molecular Processes, edited by D. R. Bates (Academic Press Inc., New York, 1962), p. 663.

[49]V. W. Hughes, J. Appl. Phys. 28, 16 (1957).

[50]Positron Annihilation, edited by A. T. Stewart and L. O. Roellig (Academic Press Inc., New York, 1967).

[51]V. W. Hughes, in Physics of the One- and Two-Electron Atoms, edited by F. Bopp and H. Kleinpoppen (North-Holland Publishing Co., Amsterdam, 1969).

[52]A. I. Alikhanov, Ya. V. Galaktionov, Ya. V. Gorodkov, G. P. Eliseev, and V. A. Lyubimov, Zh. Eksperim. i Teor. Fiz. 38, 1918 (1960) [English transl.: Soviet Phys. – JETP 11, 1380 (1960)].

[53]G. Backenstoss, B. D. Hyams, G. Knop, P. C. Marin, and U. Stierlin, Phys. Rev. Letters 6, 415 (1961).

[54]M. Bardon, P. Franzini, and J. Lee, Phys. Rev. Letters 7, 23 (1961).

[55]R. Hagedorn, Relativistic Kinematics (W. A. Benjamin, Inc., New York, 1964).

[56]R. L. Garwin, L. M. Lederman, and M. Weinrich, Phys. Rev. 105, 1415 (1957).

[57]G. W. Ford and C. J. Mullin, Phys. Rev. 108, 477 (1958).

[58]J. C. Sens, R. A. Swanson, V. L. Telegdi, and D. D. Yovanovitch, Phys. Rev. 107, 1465 (1957).

[59]R. A. Ferrell, Y. C. Lee, and M. K. Pal, Phys. Rev. 118, 317 (1960); 119, 2098 (1960).

[60]R. Prepost, Ph. D. thesis, Columbia University, 1961 (unpublished).

[61]V. Bargmann, L. Michel, and V. L. Telegdi, Phys. Rev. Letters 2, 435 (1959).

[62]Manufactured by Perfection Mfg. Co.

[63]R. L. Garwin, Rev. Sci. Instr. 24, 618 (1953).

[64]S. Penman, Rev. Sci. Instr. 30, 745 (1959).

[65]W. C. Elmore and M. Sands, Electronics (McGraw-Hill Book Co., New York, 1949).

[66]R. A. Swanson, Phys. Rev. 112, 580 (1958).

[67]M. Weinrich, Ph. D. thesis, Columbia University, 1958 (unpublished).

[68]H. S. Snyder and W. T. Scott, Phys. Rev. 76, 220 (1949).

[69]H. A. Bethe and J. Ashkin, Experimental Nuclear Physics, edited by E. Segre (John Wiley & Sons, Inc., New York, 1953), Vol. 1, p. 166.

[70]E. M. Purcell and G. B. Field, Astrophys. J. 124, 542 (1956).

[71]H. C. Berg, Phys. Rev. 137, A1621 (1965).

[72]D. McColm, V. W. Hughes, and A. Lurio, Bull. Am. Phys. Soc. 4, 82 (1959).

[73]D. McColm, Ph. D. thesis, Yale University, 1961 (unpublished).

[74]Manufactured by Penco Co.

[75]R. L. Garwin, Rev. Sci. Instr. 29, 223 (1958); 29, 900 (1958).

[76]M. A. Garstens, L. S. Singer, and A. H. Ryan, Phys. Rev. 96, 53 (1954); C. H. Townes and J. Turkevich, *ibid.* 77, 147 (1950).

[77]R. M. Mobley, in Methods of Experimental Physics, edited by V. W. Hughes and H. L. Schultz (Academic Press Inc., New York, 1967), Vol. 4B, p. 318.

[78]H. Cramér, Mathematical Methods of Statistics (Princeton University Press, Princeton, N. J., 1946); H. Cramér, The Elements of Probability Theory (John Wiley & Sons, Inc., New York, 1955).

[79]J. Orear, University of California Radiation Laboratory: Report No. UCRL-8417, 1958 (unpublished).

[80]P. K. Kabir, Nuovo Cimento 22, 429 (1961).

[81]W. A. Nierenberg, Ann. Rev. Nucl. Sci. 7, 349 (1957).

[82]J. Bailey, W. Bartl, G. von Bochmann, R. C. A. Brown, F. J. M. Farley, H. Jostlein, E. Picasso, and R. W. Williams, Phys. Letters 28B, 287 (1968).

[83]G. R. Lynch, J. Orear, and S. Rosendorff, Phys. Rev. 118, 284 (1960). A similar muon repolarization experiment in solids is described.

[84]H. S. W. Massey and R. A. Smith, Proc. Roy. Soc. London A142, 142 (1933).

[85]This calculation was done by J. M. Bailey. See J. M. Bailey and V. W. Hughes, in Atomic Collision Processes, edited by M. R. C. McDowell (North-Holland Publishing Co., Amsterdam, 1964).

[86]An improved approximation in this low-energy region would be obtained by using the modification of the PSS method given by D. R. Bates and R. McCarroll, Proc. Roy. Soc. (London) A245, 175 (1958).

[87]T. A. Green, H. E. Stanley, and Y. C. Chiang, Helv. Phys. Acta 38, 109 (1965).

[88]R. A. Mapleton, Phys. Rev. 122, 528 (1961).

[89]G. Breit and V. W. Hughes, Phys. Rev. 106, 1293 (1957).